

GOTOCORD

GOME Total Ozone Column Retrieval Development:

ESA ITT AO/1-4235/02/I-LG
ESRIN/Contract No. 16402/02/I-LG

WF-DOAS V1.0 Validation Report

Issue 1.2

M. Weber, L.N. Lamsal, M. Coldewey–Egbers, K. Bramstedt
Institute of Environmental Physics, University of Bremen

and

K. Vanicek
Czech Hydrometeorological Institute, Solar and Ozone Observatory Hradec Kralove

Address:
Institute of Environmental Physics
Institute of Remote Sensing
University of Bremen FB1
P.O. Box 330 440
D-28334 Bremen
Germany

Contact:
Mark.Weber@uni-bremen.de



January 2004

Abstract

This report summarizes the validation of the GOME total ozone derived from applying the weighting function DOAS (WF-DOAS) algorithm Version 1.0. This algorithm was developed as part of the GOTOCORD ESA project (see accompanying ATBD Report). The WF-DOAS results have been compared with selected ground-based measurements from the WOUDC (World Ozone and UV Radiation Data Centre) which collects total ozone measurements from a global network of stations. Very few of these stations carry out simultaneous measurements by Brewer and Dobson spectrometers over an extended period (three years or more). Simultaneous Brewer and Dobson measurements from Hradec Kralove, Czech Republic (50.2°N, 15.8°E) and Hohenpeissenberg, Germany (47.8°N, 11.0°E) covering the period 1996-1999 have been compared with our GOME results and particular attention is paid to the differences between the two ground spectrometer types and GOME.

Contents

Abstract	2
1 GOME WF-DOAS total ozone and the validation datasets	4
1.1 WF-DOAS settings	4
1.2 GOME Data Processor Version 3.0	5
1.3 WOUDC total ozone data set	6
1.4 Dobson and Brewer instrumentation	6
2 Comparison with simultaneous Brewer and Dobson	7
2.1 GOME validation at Hohenpeissenberg and Hradec-Kralove	7
2.2 Discussion	11
2.3 Long-term validation 1996–2003	13
3 Comparison with the WOUDC data set	16
3.1 Selected stations: from north to south	16
3.2 Statistical analysis	19
3.3 Ozone hole observation	22
4 Summary and Conclusion	26
Acknowledgement	27
References	28
Appendix	30
A List of stations from the WOUDC data base	30
B Summary plots for GOME-WOUDC comparison in various regions	31
B.1 Northern hemisphere polar region, 60°N–90°N	32
B.2 Northern hemisphere mid-latitude, 25°N–60°N	34
B.3 Tropics, 25°S–25 °N	36
B.4 Southern hemisphere mid-latitude, 25°S–60°S	38
B.5 Southern polar region, 60°S–90°S	40

1 GOME WF-DOAS total ozone and the validation datasets

1.1 WF-DOAS settings

In this report we validate Version 1.0 of the GOME WF-DOAS total ozone. Details of the weighting function DOAS fitting has been summarized in the ATBD document and only the basic settings defining Version 1.0 are briefly given here as reference. In a few cases some modified settings have been tested and validated and these cases are clearly identified throughout the report.

The following settings apply to Version 1.0 WF-DOAS:

- spectral fitting window: 326.6–335.0 nm
- fitting parameters:
 - ozone vertical column (WF)
 - temperature shift (WF)
 - under-sampling correction
 - Ring SCD (including ozone filling-in)
 - NO₂ SCD
 - BrO SCD
- Burrows *et al.* (1999) ozone cross-section shifted by +0.017 nm
- Fraunhofer fitting (wavelength calibration of daily solar GOME reference to Kitt Peak FTS solar atlas from Kurucz *et al.* (1984))
- shift and squeeze of wavelength axis only for earthshine spectrum
- cubic polynomial subtracted in the fit
- Lambertian equivalent reflectivities (377.6nm) taken as effective albedo of the scene,
- cloud-top-height and cloud cover fraction derived using FRESCO (Koelemeijer *et al.*, 2001). Effective height is determined from the cloud-information
- ghost vertical column correction from TOMS V8 zonal monthly mean climatology
- a-priori ozone profile shape from total ozone dependent TOMS V7 ozone and temperature climatology (Wellemeyer *et al.*, 1997)

The weighting functions (ozone and temperature) and reference intensities are taken from look-up-tables (LUT) consisting of radiative transfer model calculations that uses the TOMS V7 ozone and temperature profile climatology as input (Wellemeyer *et al.*, 1997). This climatology is divided into three zones, low-latitudes (tropics), mid-latitudes, and polar region without distinction of hemispheres. The O₃ and NO₂ cross-sections (Burrows *et al.*, 1998, 1999) have been shifted by +0.017 nm following the recommendation by the GDP V3.0 implementation report (GDP V3 VALREPORT, 2002).

The V1.0 retrieval was done twice by selecting two different climate zones for each station. In the extra-tropical region, mid-latitude and high latitude profiles were selected, while in the tropics, low-latitude and mid-latitude profiles were selected. The reason for choosing two different climate zones is to estimate its impact

on the retrieved total ozone. Since ozone in the lowermost stratosphere has a photochemical lifetime of several months, the ozone distribution from different climate regions can well extend into other zones. For instance, tropical or sub-tropical streamers bring air-masses with low ozone into mid- and high latitudes (phenomenon of mini-holes) and also polar air-masses can move to lower latitudes (polar streamers) (Waugh, 1997; Weber *et al.*, 2002). It is most probable that in each zonal region profile shape information from air-masses originating in other zones are present.

Only the regular swath width data with 320 km (across scan) times 40 km (along-track) that represents the vast majority of GOME observations were analyzed.

1.2 GOME Data Processor Version 3.0

The current operational data version for GOME total ozone is Version 3.0 (short GDP V3.0) that uses the standard DOAS approach of slant column fitting and airmass factor correction to obtain the total column amounts. The Version 3.0 has been introduced in November 2002 and are distributed by ESA to the user/scientific community. The V3.0 data was used as initial guess in the iterative WF-DOAS retrieval scheme. In this report the changes from the operational version to our WF-DOAS is investigated to obtain a better insight into the performance of the new algorithm.

The following settings applies to GDP V3.0 (GOME LVL2, 2000; GDP V3 VALREPORT, 2002):

- spectral fitting window: 325–335 nm
- fitting parameters:
 - ozone slant column density for two temperatures (SCD)
 - Ring SCD without molecular-filling in (Chance and Spurr, 1997)
 - under-sampling correction
 - NO₂ SCD
- Burrows *et al.* (1999) ozone cross-section shifted by +0.012 nm
- Shift and squeeze of wavelength axis only for solar reference spectrum.
- quadratic polynomial subtracted in the fit
- cloud cover determination from oxygen A-band (ICFA: Initial Cloud Fitting Algorithm)
- iterative airmass factor at 325 nm using a neural network scheme and TOMS V7 ozone profile climatology. Combination of cloud and clear-sky AMFs for total ozone conversion is used
- ghost vertical column correction from TOMS V7 ozone climatology

Major changes from GDP V2.7 to V3.0 was 1) the use of two ozone cross-sections at different temperature in the fitting, 2) replacement of GOME FM Ring-spectrum (based upon cross-polarization measurements) by a theoretical Chance and Spurr (1997) Ring spectrum, and 3) an introduction of an iterative AMF scheme that uses TOMS V7 climatology. The two temperature fits accounts for the ozone temperature variation, but in a different way as done in WF-DOAS, where the temperature shift weighting function provides radiance changes due to a constant shift in the entire profile. For more details related to GDP V3.0, the reader is referred to GDP V3 VALREPORT (2002). First validation results seem to indicate that seasonal differences to ground-based data have been reduced significantly by nearly a half as compared to V2.7. In addition improvements in the SZA and total column dependencies of the differences have been found (Lambert *et al.*, 1999; Lambert, 1995; GDP V3 VALREPORT, 2002).

1.3 WOUDC total ozone data set

The World Ozone and Ultraviolet Radiation Data Centre (WOUDC) is a project of the Experimental Studies Division of Environment Canada for the World Meteorological Organisation (WMO). It is one of five World Data Centres which are part of the Global Atmosphere Watch (GAW) programme which in turn is part of the World Meteorological Organisation (WMO). The ozone data archive at WOUDC contains lidar and ozone-sonde vertical profiles, Umkehr data, and total column ozone from Dobson and/or Brewer spectrometers among other data (Hare and Fioletov, 1998).

In Table 1 of Appendix A the set of stations (about 43) that have been selected in the validation are listed. The majority of them are located in the northern hemisphere. It is a well-known problem that southern hemispheric as well as tropical stations are rather sparse. This data set has been used in a previous validation study related to GDP V2.7 total ozone, TOMS V7 total ozone, and integrated columns from GOME ozone profiles (Hoogen *et al.*, 1999; Bramstedt *et al.*, 2003).

For all stations GOME overpasses have been identified for the period 1996-2003. Pairs of collocated measurements from GOME and from the ground were selected using the criteria that both are from the same day and the distance between the center coordinate of the GOME ground pixel is 300 km or less. Only the nearest GOME pixel was selected at a given date. The groundbased data represents daily averages.

1.4 Dobson and Brewer instrumentation

The majority of the total ozone data contained in the WOUDC database are from Dobson spectrophotometer measurements. The Dobson spectrophotometer is a double monochromator with the first prism acting as a dispersing element and the second recombining the wavelength pair on to a photomultiplier. A chopper allows the alternating measurements of the wavelength pair with a single detector (Dobson, 1931, 1968). For the standard analysis (WMO-GAW) the A (305.5/325.5 nm) and D (311.5/332.4) wavelength pairs are used to derive total ozone (Staehelin *et al.*, 2003). At low solar elevation the D-pair can be combined with the C-pair 311.5/332.4 nm. This instrument can be operated in direct-sun mode and be used for zenith sky measurements. Most reliable results are obtained in direct-sun (AD pairs) with a precision of 1% using a diffuser plate. Accuracy may be lower due to systematic errors, for instance coming from uncertainties in cross-sections (Bass-Paur are used in the standard retrieval). Under cloudy conditions the error in the zenith-sky results can raise from 3% up to 7% (low clouds) in zenith sky measurements (R.D. Evans, NOAA, personal communication). First measurements with the Dobson instruments have been reported in the twenties (Dobson, 1931) and some of the longest time series are provided by the Dobson instruments (Staehelin, 1998).

Since the early eighties Brewer grating spectrometers have been installed at several stations (Kerr *et al.*, 1985). It is a modified Ebert type grating spectrometer which can be operated in single (*single Brewer*) or double monochromator (*double Brewer*) configuration. This instrument uses five wavelengths in the spectral range 306.3 and 320.1 nm to form several wavelength pairs for the standard ozone retrieval. Besides ozone, NO₂, SO₂, and UV-B radiation can be measured. Particularly SO₂ interferes in the ozone retrieval and has to be corrected for, particularly, in an urban environment. Both direct-sun and zenith-sky measurements are possible.

The procedure for calibrating Dobson spectrophotometers has been highly standardized using traveling reference instruments and by many inter-comparison campaigns under the guidance of WMO (Basher, 1995; Grass *et al.*, 1994, see for instance). The Brewer network is much smaller and the calibration of these instruments rely more on the efforts of the individual stations and comparisons with large number of instruments have not been done so far (Staehelin *et al.*, 2003).

2 Comparison with simultaneous Brewer and Dobson

Only very few stations provide simultaneous measurements from Brewer and Dobson spectrometers covering an extended period. Two such stations are Hohenpeissenberg (MOHp), Germany, 47.8°N, and Hradec-Kralove, Czech Republic, 50.2°N. Both stations in collaboration acts as the Regional Dobson Calibration Centre for Europe. They have been operating a single Brewer and Dobson throughout the GOME period 1995-2003 and this data set is very valuable in evaluating the new GOME algorithm. Because of different wavelengths used in all three instruments GOME, Brewer, and Dobson, results may differ. Also seasonal dependence on the retrieved ozone may differ. The standard retrieval procedure as defined by WMO-GAW, for instance, does not correct for the ozone temperature variation in contrast to the GOME retrieval algorithms GDP V3.0 and WF-DOAS V1.0.

2.1 GOME validation at Hohenpeissenberg and Hradec-Kralove

For both stations a maximum collocation radius of 160 km between the center of the GOME pixel and station location was allowed and measurements had to take place the same day. At a given day only the closest match within that radius was taken. Brewer and Dobson data were provided as daily averages. All Dobson measurements and the Hradec-Kralove Brewer are limited to direct sun measurements that are considered most reliable. Hohenpeissenberg Brewer data also contain zenith-sky measurements.

Figure 2.1 shows the comparison between WF-DOAS V1.0 and Hohenpeissenberg Brewer as a function of the day in the year (1996–1999). The top panels shows the annual cycle of total ozone with maximum ozone in spring and minimum in fall, the bottom panel the difference in percent. The WF-DOAS results have a bias of 0.4% and a $\pm 0.5\%$ variability over the annual cycle with slightly higher values in winter (JFM) than in summer/fall. The 1σ RMS in the differences is 2.3%. The comparison of GDP V3.0 with MOHp Brewer data is shown in Fig. 2.2 and the bias between both datasets is on average -0.5% and, therefore, WF-DOAS V1.0 is 0.9% higher than GDP V3.0. The annual variability in the GDP differences with respect to the Brewer is about $\pm 1.5\%$ with a maximum in spring and minimum in fall. The 1σ RMS of the differences is 3.2% and is 1% higher than the corresponding RMS in the WF-DOAS differences.

The comparison of the GOME WF-DOAS V1.0 and GDP V3.0 with the Dobson measurements is shown in Figs. 2.3 and 2.4, respectively. The RMS scatter in the differences are similar for both data as observed with the Brewer (2.3% and 2.9%, respectively). The WF-DOAS exhibits a somewhat stronger seasonal cycle of $\pm 1\%$ when compared to Dobson with a maximum differences of +1.5% during winter and 0% difference in summer. The GOME GDP V3.0 shows a similar seasonal variation of $\pm 1\%$ with respect to the MOHp Dobson and slightly enhanced with respect to Brewer.

Overall little seasonal variation is seen in the differences between both GOME data versions and the ground-based instruments (less than $\pm 1.5\%$). The RMS scatter in the differences to the ground-based data has drastically improved with WF-DOAS despite the fact that some of the differences may be also in part due to different air-masses viewed by satellite and ground instrumentations. The WF-DOAS results appear to exhibit only a very small seasonal variation with respect to the Brewer.

Similar conclusions can be derived from the comparison with the ground-based data from Hradec-Kralove. In Fig. 2.5 different combinations of differences between satellite and ground-based data are shown. The top two panels show differences of WF-DOAS with respect to Brewer and Dobson, while the lowermost two panels show differences of GDP V3.0 with each of the ground instruments. The middle panel depicts the differences between average Dobson and Brewer results from the same day.

The WF-DOAS bias with respect to Brewer is less than 0.2% and the very weak seasonal cycle of $\pm 0.5\%$ like

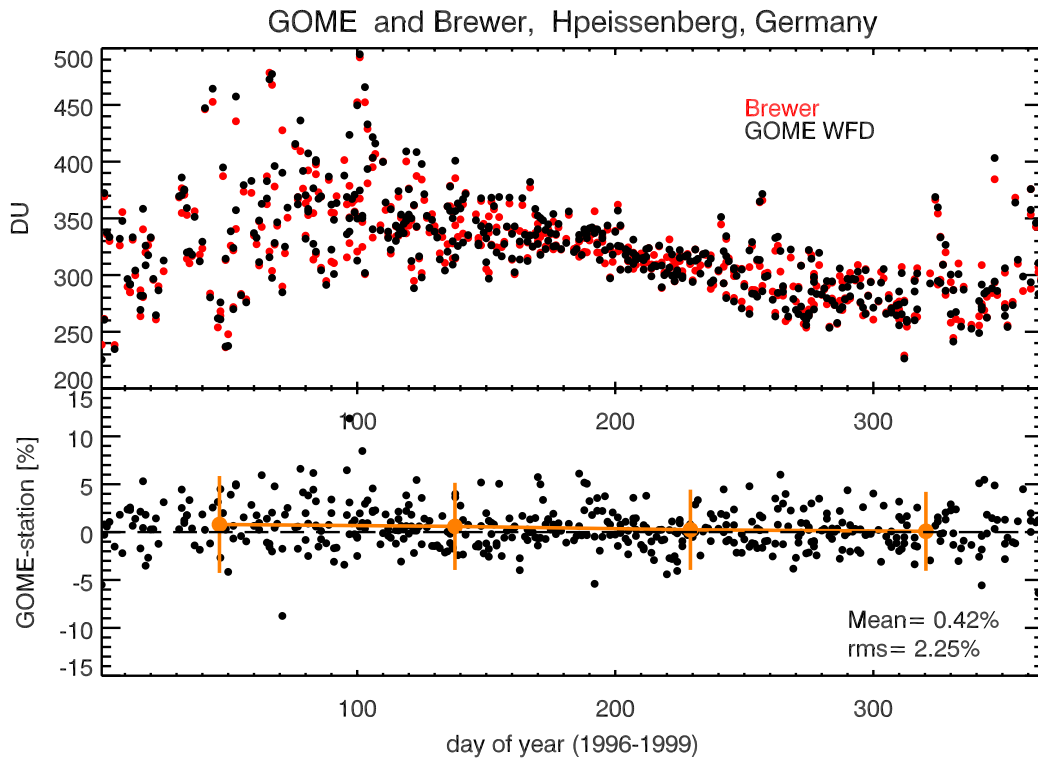


Figure 2.1: Top panel: Collocated GOME WF-DOAS V1.0 and Brewer total ozone from Hohenpeissenberg, bottom panel: Differences in percent. Orange points mark the three month average in the differences and bars the 2σ RMS.

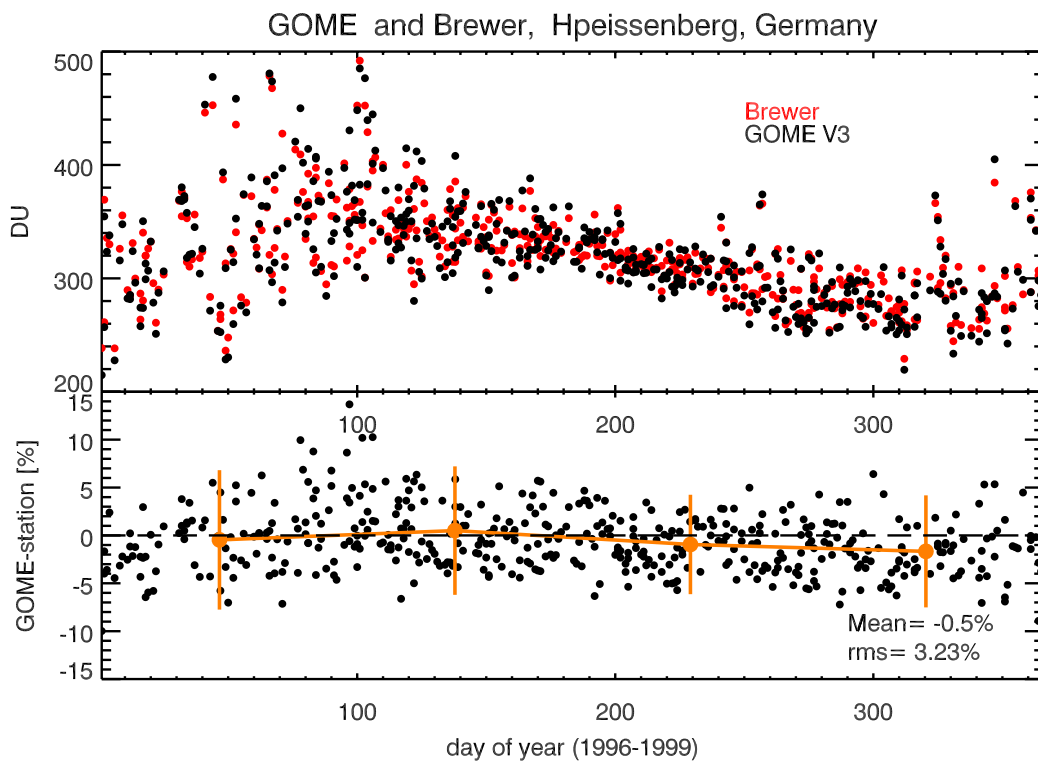


Figure 2.2: Same as Fig. 2.1, but with GDP V3.0 data, the current operational ESA product.

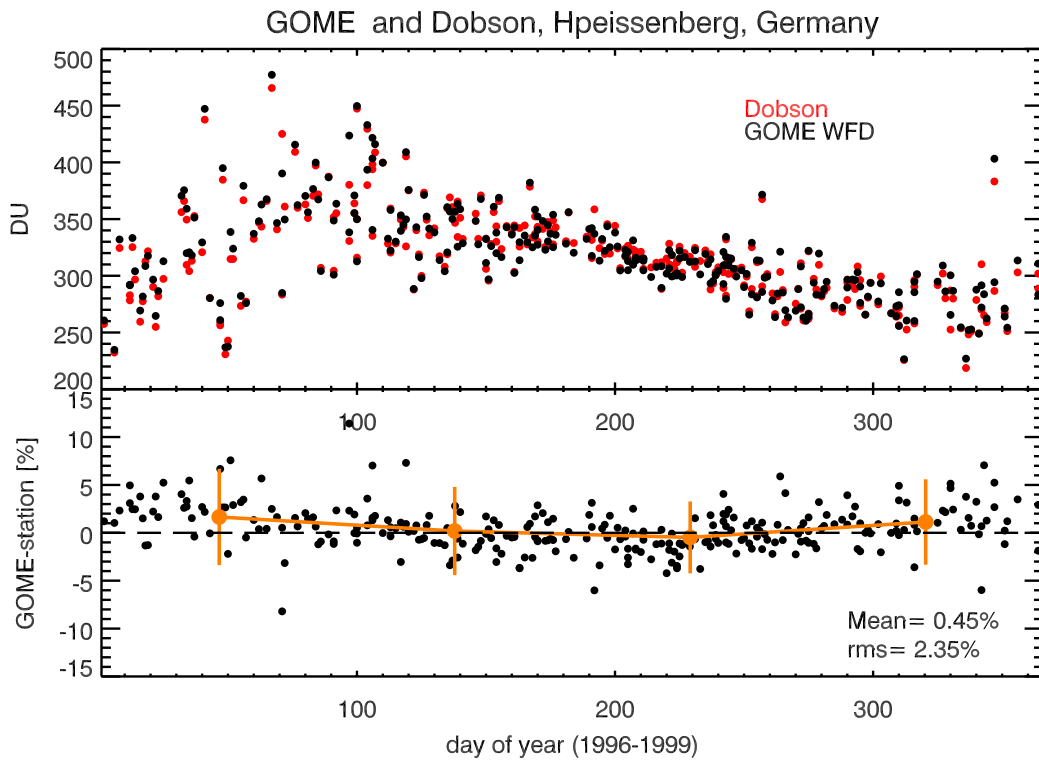


Figure 2.3: Same as Figure 2.1 but shown for collocated WF-DOAS and Dobson measurements at Hohenpeissenberg. Only direct-sun measurements from the Dobson are shown here.

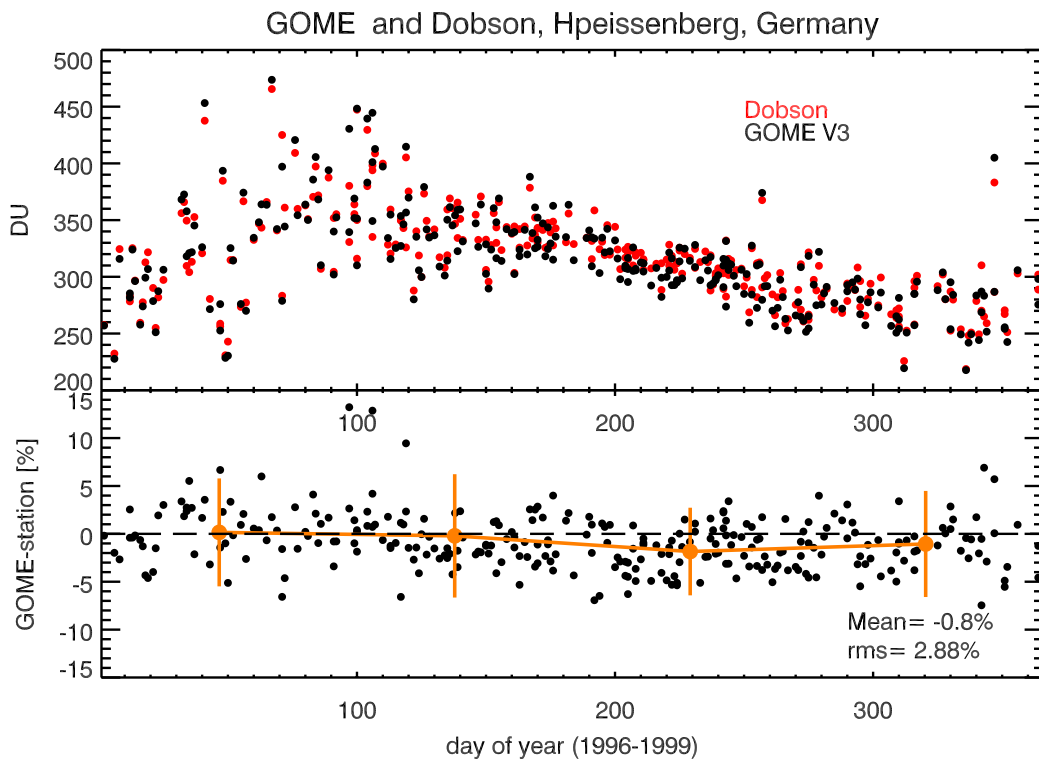


Figure 2.4: Same as Figure 2.1 but shown for collocated GDP V3.0 and Dobson direct sun measurements at Hohenpeissenberg.

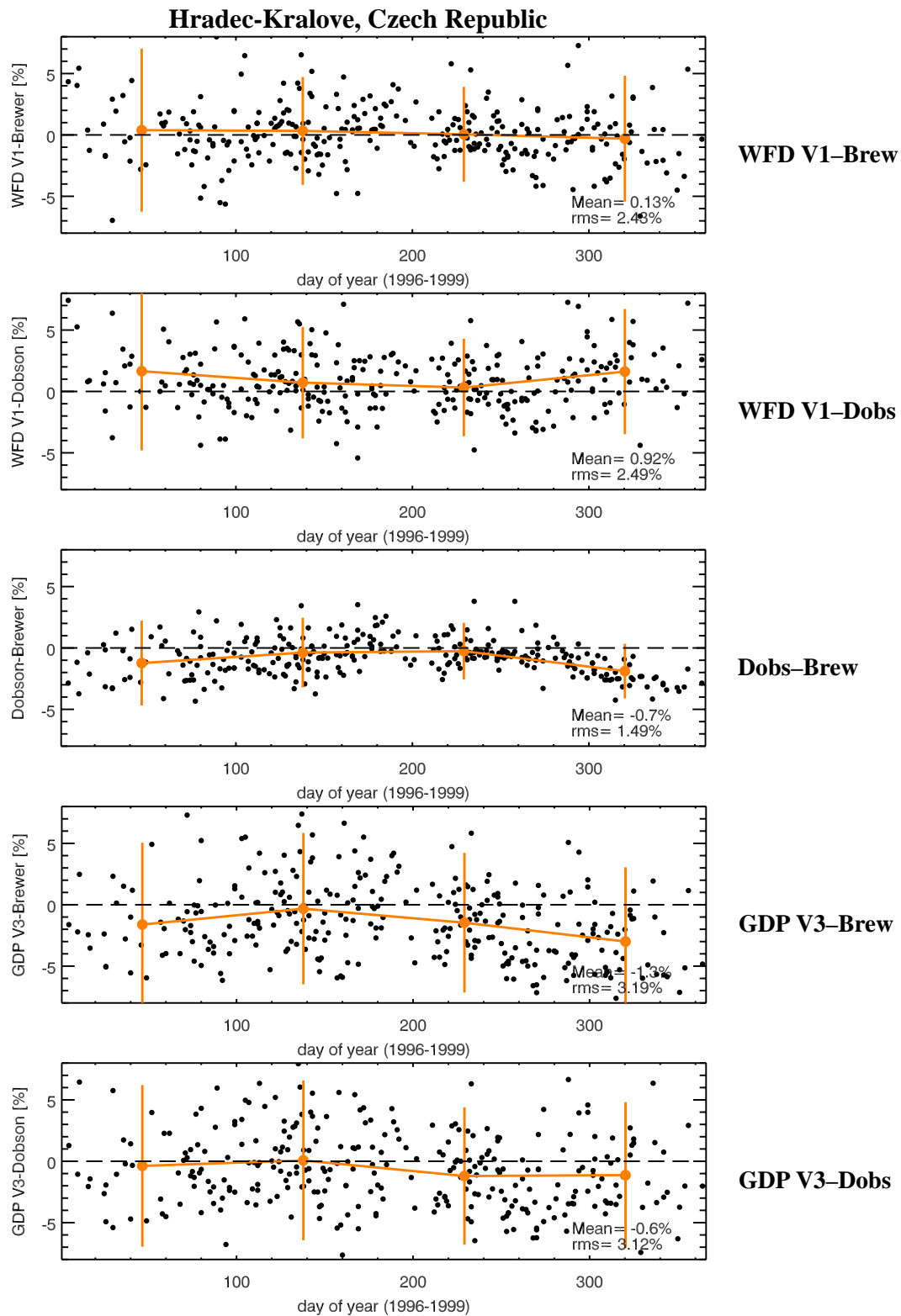


Figure 2.5: Annual course of differences between GOME (WF-DOAS V1 and GDP V3.0), single Brewer, and Dobson data at Hradec-Kralove shown for (almost) all possible pair combinations.

Table 2.1: Differences of WF-DOAS V1.0 with Brewer and Dobson in percent (bracket: RMS scatter) for the period 1996–1999. I: Jan-Mar, II: Apr-Jun, and so on.

Instrument	Station	All season	I	II	III	IV
Brewer	MO Hohenpeissenberg	0.42 (2.3)	0.8 (2.5)	0.6 (2.3)	0.2 (2.1)	0.1 (2.1)
	Hradec Kralove	0.13 (2.4)	0.5 (3.3)	0.3 (2.2)	0.1 (1.9)	-0.4 (2.6)
Dobson	MO Hohenpeissenberg	0.45 (2.4)	1.7 (2.5)	0.2 (2.3)	-0.5 (1.9)	1.1 (2.3)
	Hradec Kralove	0.93 (2.5)	1.7 (3.2)	0.7 (2.3)	0.3 (2.0)	1.6 (2.6)

in the MOHp data is evident here. A somewhat larger seasonal variation is observed if compared to Dobson ($\pm 1\%$). This is in line with the earlier comparison to MOHp. Note that the percentage scale is larger in these plots as compared to the MOHp plots; the RMS scatter of the differences remains about the same. Again the scatter in the WF-DOAS differences are significantly lower than for GDP and noticeable in the plots. The GDP V3.0 results show seasonal variation on the order of $\pm 1.5\%$ in the Brewer differences and smaller in the Dobson differences.

When comparing data from both stations it is noticeable that the Hradec-Kralove Dobson is 0.5% lower on average than the same instrument at MOHp. A new set of calibration settings were introduced in Hradec-Kralove in 1997 that were not adopted at MOHp (U. Köhler, DWD, personal communication) and that may explain this bias. The change in the calibration settings is also noticeable from the longterm times series in the Dobson-Brewer differences at Hradec-Kralove that showed less variability in 1996 and earlier (Staehelin *et al.*, 2003, see Fig. 5).

2.2 Discussion

Comparisons of both satellite data versions with two different ground-type instruments at each station provide a quite consistent picture. Both satellite algorithm show weak seasonal dependence in the differences; agreement is particularly well between WF-DOAS V1.0 and Brewer, with almost negligible seasonal variation in the observed differences (see also Table 2.1). The RMS scatter in the differences is smaller using WF-DOAS (in both Dobson and Brewer comparisons) than for GDP indicating excellent performance of the WF-DOAS algorithm. The GDP V3.0 tends to agree slightly better with Dobson than Brewer.

The variability in the observed differences between Dobson and Brewer are on the same order as observed in the differences between different GOME algorithms. The major contribution to this seasonal cycle in Dobson-Brewer differences is due to the use of different wavelength pairs in both instruments to retrieve ozone. Particularly, the D pair ratio of the O_3 cross-sections (317.6/339.8 nm) as used by the Dobson shows the largest temperature dependence of all ratios used in the standard retrieval by both instruments (Staehelin *et al.*, 2003). However, a fixed temperature (226.9 K) ozone cross-section is applied in the standard retrieval so that the stratospheric temperature variation with season is not accounted for.

Particularly in winter the stratospheric temperature are below the fixed ozone temperature that may explain the larger differences between Dobson and Brewer in winter. For a typical ozone/temperature variability at mid-latitude station a sensitivity of $+1.3\%/10$ K and $+0.7\%/10$ K in ozone change for Dobson and Brewer, respectively, has been estimated (Komhyr *et al.*, 1993; Kerr *et al.*, 1988). Up to two-third of the differences between Dobson and Brewer can be corrected for by using the proper effective ozone temperature, for instance derived from collocated sonde measurements (Staehelin *et al.*, 2003). The remaining uncertainty comes most likely from the forward scattering (stray-light) into the Dobson spectrophotometer in direct-sun observation mode, that has a larger field-of-view than the Brewer spectrometers. Also, single Brewers suffer more signifi-

Table 2.2: Differences between WF-DOAS V1.0 and Hradec-Kralove Brewer and Dobson, respectively, before and after temperature correction applied to groundbased data.

Hradec-Kralove	mean	I	II	III	IV
WF-DOAS - Brewer [%]	0,13	0,5	0,3	0,1	-0,4
WF-DOAS - Brewer T corr [%]	-0,24	-0,2	0,1	0,1	-1,1
WF-DOAS - Dobson [%]	0,93	1,7	0,7	0,3	1,1
WF-DOAS - Dobson T corr [%]	0,23	0,4	0,4	0,3	0,3

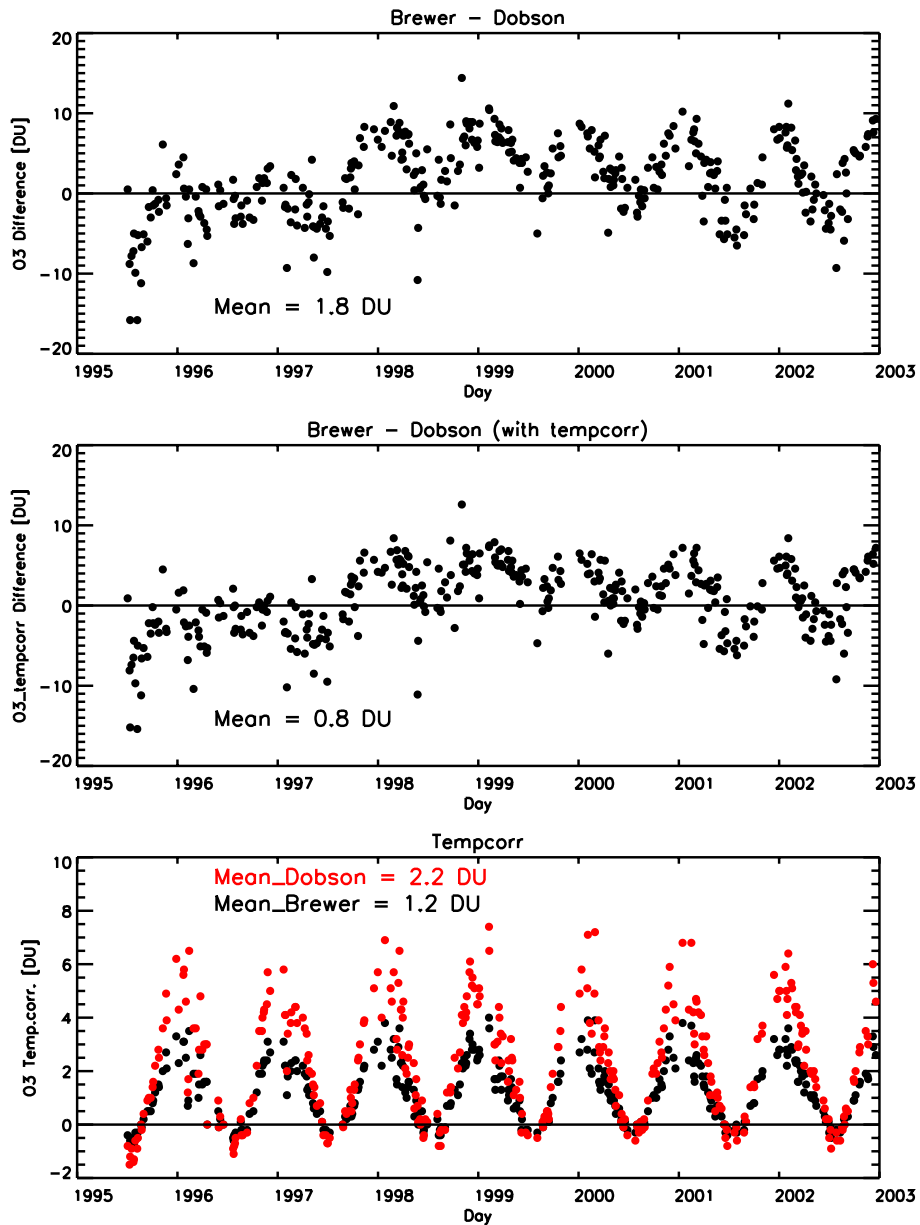


Figure 2.6: Differences between DS Brewer and Dobson at Hradec-Kralove without ozone temperature correction (top) and after ozone temperature correction (middle panel) applied in the retrieval from both ground instruments. The bottom panel shows the net temperature correction for Dobson (red) and Brewer (black) in DU. Only Dobson and Brewer data measured within a ten minute time difference are shown here. If more than one measurement was taken at a given day, daily averages were calculated.

cantly from straylight than double Brewers. The straylight error occurs at high solar zenith angles (in winter) and it goes in the same direction as the ozone temperature error (U. Köhler, DWD Hohenpeissenberg, personal communication). Both effects can lead to a maximum of $\pm 2\%$ variability between both types of ground-based instruments. In zenith-sky measurements that variability becomes smaller (Vanicek, 1998).

In Figure 2.6 the differences between Brewer and Dobson measured simultaneously within ten minutes in Hradec-Kralove are shown without temperature correction (top panel, standard retrieval) and after a temperature correction has been applied (middle panel). The ozone temperature was determined from the ozone weighted average temperature profile derived from sonde ascents in Prague and Hohenpeissenberg (Vanicek *et al.*, 2003). The temperature correction in Dobson units as a function of time is shown in the bottom panel of Fig. 2.6. In winter the temperature correction can be up to 8 DU (3 DU for Brewer). The annually averaged correction for the Hradec-Kralove Dobson is about 1.2 DU for Brewer and 2.2 DU for the Dobson instruments. A residual seasonal variation in the Brewer-Dobson difference time series is still evident after ozone temperature correction. The modification in the calibration setting of the Dobson instrument is clearly noticeable in the Brewer-Dobson difference that exhibits a jump by about 3-4 DU in 1997. Table 2.2 shows an updated comparison to ozone temperature corrected ground-based data. The temperature correction to the results in Table 2.1 were obtained by determining the average difference in percent from the bottom panel in Fig. 2.6 for the various seasons labelled I to IV. The annual mean difference between WF-DOAS and Brewer has been reduced to -0.2% , while difference to Dobson has been lowered to $+0.2\%$. The seasonal variation is now clearly minimised with respect to both ground instruments.

A variability of the GOME differences for both WF-DOAS V1.0 and GDP V3.0 of up to 1.5% is clearly within the uncertainties of the ground-based instruments. The better agreement of WF-DOAS with Brewer (variability of below $\pm 0.5\%$) is an indication that the temperature correction in the new GOME algorithm works very well at mid-latitude sites.

2.3 Long-term validation 1996–2003

For selected stations the validation has been extended over the eight year life span of the GOME instrument. This long-term comparison has been carried out with the Brewer and DS Dobson measurements from Hohenpeissenberg, 48°N (courtesy Ulf Köhler, DWD, MOHp Hohenpeissenberg) and Lauder, 45°S (courtesy of Bob Evans, NOAA). The WF-DOAS time series along with the Lauder Dobson data is shown in Fig. 2.7. All measurements from zenith-sky and direct-sun groundbased data have been included. Apart from a bias of $+0.8\%$ for the entire time period no seasonal variation is seen in the comparison of WF-DOAS V1.0, except for a brief period in 2002, where the differences increased to 4% . The most likely explanation of this effect is the lack of updated mean solar spectrum in the GOME level 1 data product during the period between October 2001 and October 2002. A re-evaluation of the data using proper solar reference data is underway. The bottom panel in Figure 2.7 shows the same comparison but with GDP V3.0, where a distinct seasonal cycle is evident for all years.

A similar comparison is shown in Fig. 2.8 for the Brewer data from Hohenpeissenberg. No distinct seasonal cycle is observed in the differences with WF-DOAS V1.0. As shown earlier GDP V3.0 exhibits a seasonal signature in the differences. On average the difference between WF-DOAS and the German Brewer is 0.6% , nearly identical to the value observed with the Lauder time series. Again the significant reduction in the sRMS scatter of the differences for WF-DOAS is striking (2.5% 1σ vs 3.5% for GDP V3.0).

From this limited comparison with two stations up to 2003, it can be concluded that the DOAS retrieval does not suffer from the optical degradation that have altered the radiometric accuracy of the GOME instrument particularly in later years (Tanzi *et al.*, 2001).

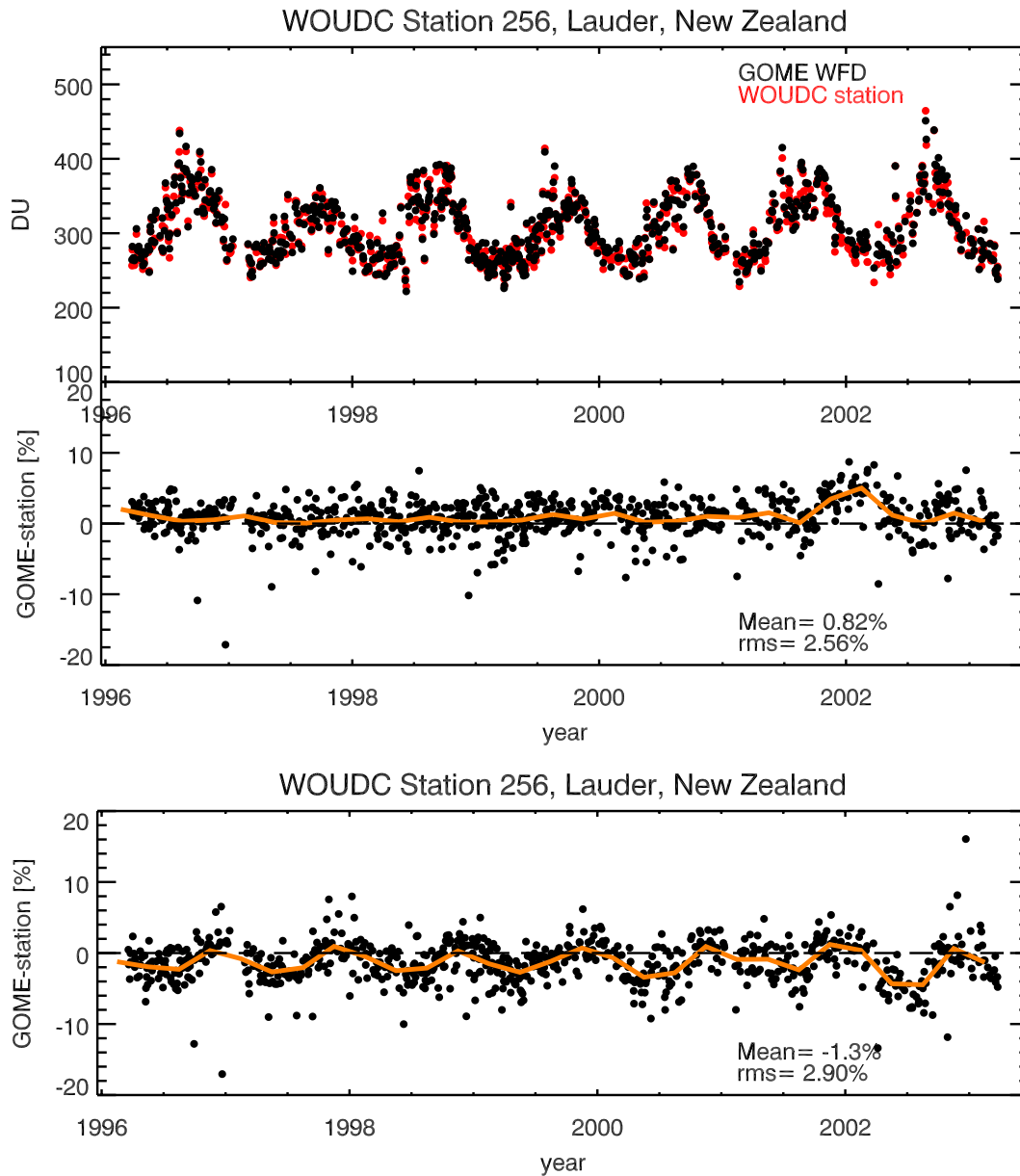


Figure 2.7: Time series of collocated GOME WF-DOAS V1 (black) and Dobson data (red) from Lauder, New Zealand, during the period between March 1996 and March 2003 (top panel). Middle panel shows the difference in percent between GOME and Dobson for WF-DOAS V1.0, while bottom panel shows the difference of GDP V3.0 and Dobson.

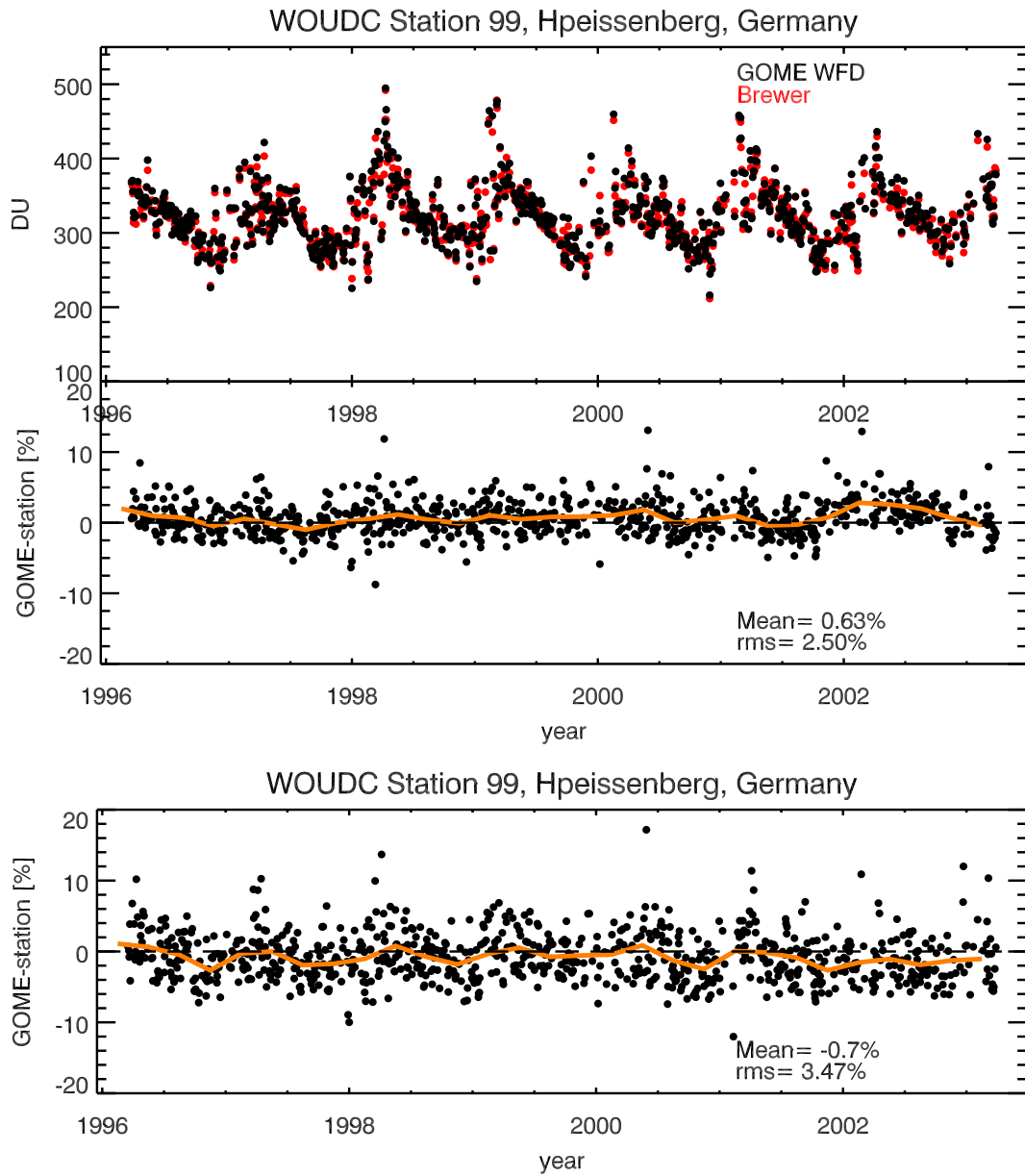


Figure 2.8: Time series of collocated GOME WF-DOAS V1 (black) and Brewer data (red) from Hohenpeissenberg, Germany, from March 1996 until March 2003 (top panel). Middle panel shows the difference in percent between GOME and Dobson for WF-DOAS V1.0, while bottom panel shows the difference of GDP V3.0 and Dobson.

3 Comparison with the WOUDC data set

3.1 Selected stations: from north to south

About 45 stations have been selected from the WOUDC data base for validating WF-DOAS V1.0. The maximum collocation radius was here set to 300 km (between centre of GOME footprint and station) and only the nearest GOME overpass was used at given day. The same data set has been used in a recent paper validating the GDP V2.7 (Bramstedt *et al.*, 2003). For each climate zone a representative station has been selected and the differences are shown as a function of time from 1996 to 1999 in Figure 3.1. The stations are from north to south; Resolute (Canada, 75°N), Boulder (USA, 40°N), Singapore (1°N), Comodoro Rivadavia (Argentina, 46°S), and Syowa, the Japanese station in Antarctica (69°S). Also shown are the three month mean time series (orange line) in order to visualize possible seasonal variability and a longterm drift in the data. Data shown here have been analyzed with the appropriate ozone climatology (tropics, mid-latitude, and polar). As with earlier versions of the GOME total ozone and in the previous sections, the station time series shows no significant long-term drift (GDP V3 VALREPORT, 2002; Bramstedt *et al.*, 2003).

Both mid-latitude stations in both hemispheres as well as the data from Singapore have an average bias over the four year period that is well below $\pm 0.5\%$. Except for Boulder and the polar stations no seasonal signature is detectable. The Boulder difference series has a distinct seasonal cycle of up $\pm 1.5\%$ starting in 1997 that is not apparent in 1996. As discussed in the previous section it could be related to the change in calibration settings that many stations introduced to their Dobson spectrophotometers in 1997. The seasonal signature in Boulder is quite similar to that observed with Hradec-Kralove and MoHP Dobsons with maximum in winter and minimum in summer.

In Comodoro Rivadavia, Argentina, a seasonal signature is not clearly discernible, except for occasional larger deviations that are not repeated in other years. This is most likely related to interruptions in measurements in winter, so that only few data contributed to the three month average as in 1997 and 1999. The five stations shown in Fig. 3.1 are also plotted as a function of the annual cycle (Fig. 3.2). The lack of seasonal cycle in the Argentina data differences becomes clearer.

The two stations in the the south and north polar station (Syowa and Resolute) show a distinct annual cycle in the differences to Dobson. Average differences in spring/summer are quite low (below 1%) but can increase to +5% close to the polar night terminator. It is remarkable that this pattern is symmetric about the polar night period, although total ozone under ozone hole conditions in spring is much lower than in fall (see Figure 3.3). The large gradients in ozone observed near the polar vortex edge is responsible for the larger scatter in the SH spring, because both GOME and surface instrument do not look at the same airmass. This general increase in the vicinity of the polar night period is a feature also observed with GDP Version 3.0.

At low solar elevation Dobson instruments suffer from forward scattered stray light and therefore may underestimate the total column. At the same time the intensity of the scattered light decreases and signal-to-noise increases in the GOME radiances and error also gets larger. It is generally difficult for UV/vis instruments to operate in near twilight condition. To reach a better understanding of differences between satellite (TOMS) and ground-based instruments at high-latitudes a measurement campaign involving two Dobson and three Brewer instruments were carried out in Fairbanks, Alaska, in March/April 2001. Against the world standard (Instrument D83, AD pair, direct sun), all Brewer instruments as well as integrated sonde profiles have shown a percent difference of +3 to +4% with respect to the world standard (Staehelin *et al.*, 2003). The Fairbanks direct-sun Dobson results showed a difference of -1.3% using the AD pair and, when using proper ozone temperature and the CD Pair, a 3.5% difference with respect to D83 was found. In winter/early spring 1998 and 1999, Arctic ozone levels were similar to those in 2001 during the TOMS3-F campaign (*warm stratospheric Arctic winter*, see also Fig. 3.3) and a difference of +2 to +4% is observed in late winter/early spring with respect to the Resolute Dobson, that goes in the same direction as the Brewer–Dobson difference observed in Fairbanks.

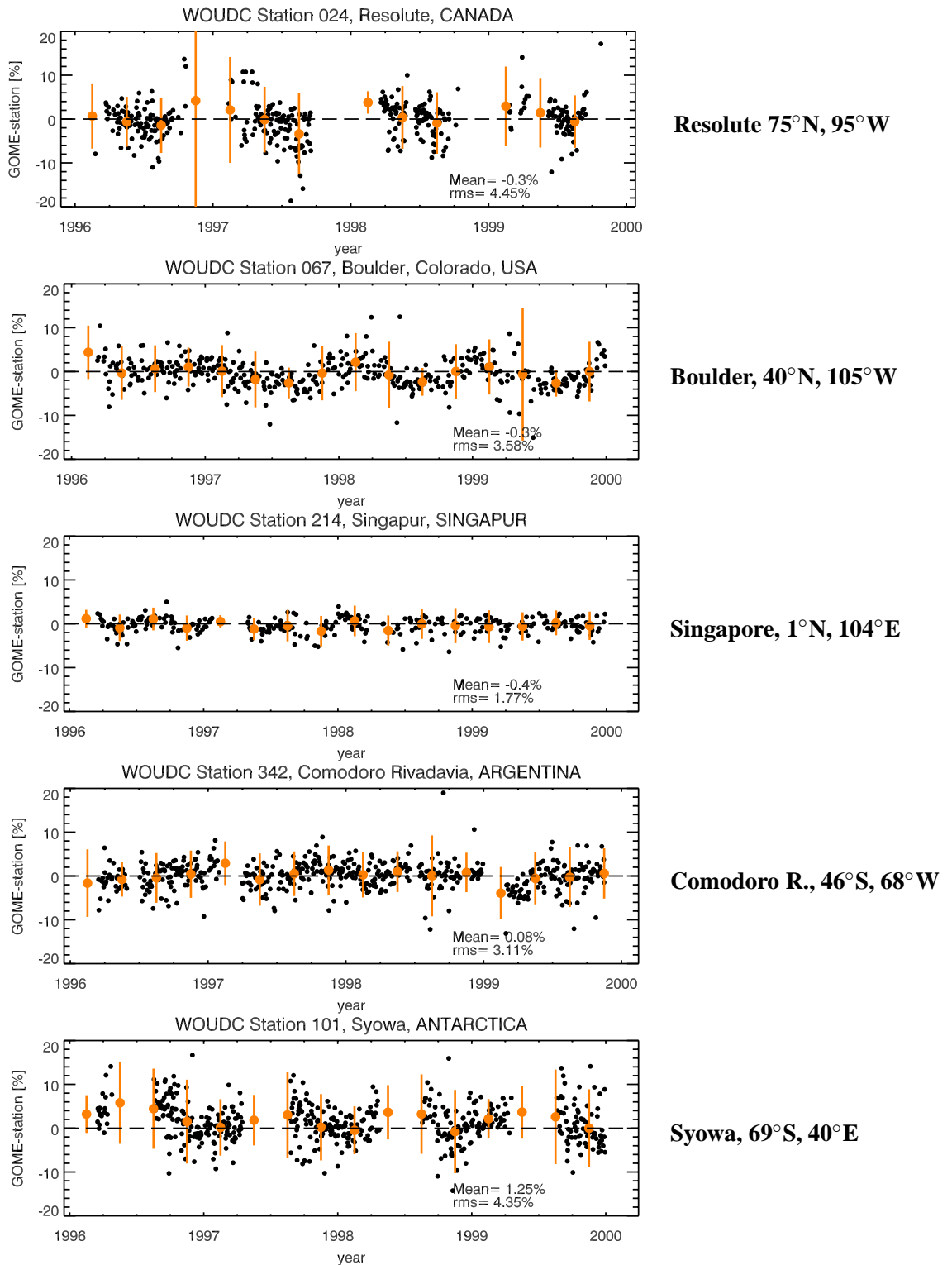


Figure 3.1: Difference between GOME WF-DOAS V1.0 and various Dobson stations distributed from North to South between 1996 and 1999. Points mark three month averages and error bars the 2σ RMS in the observed differences.

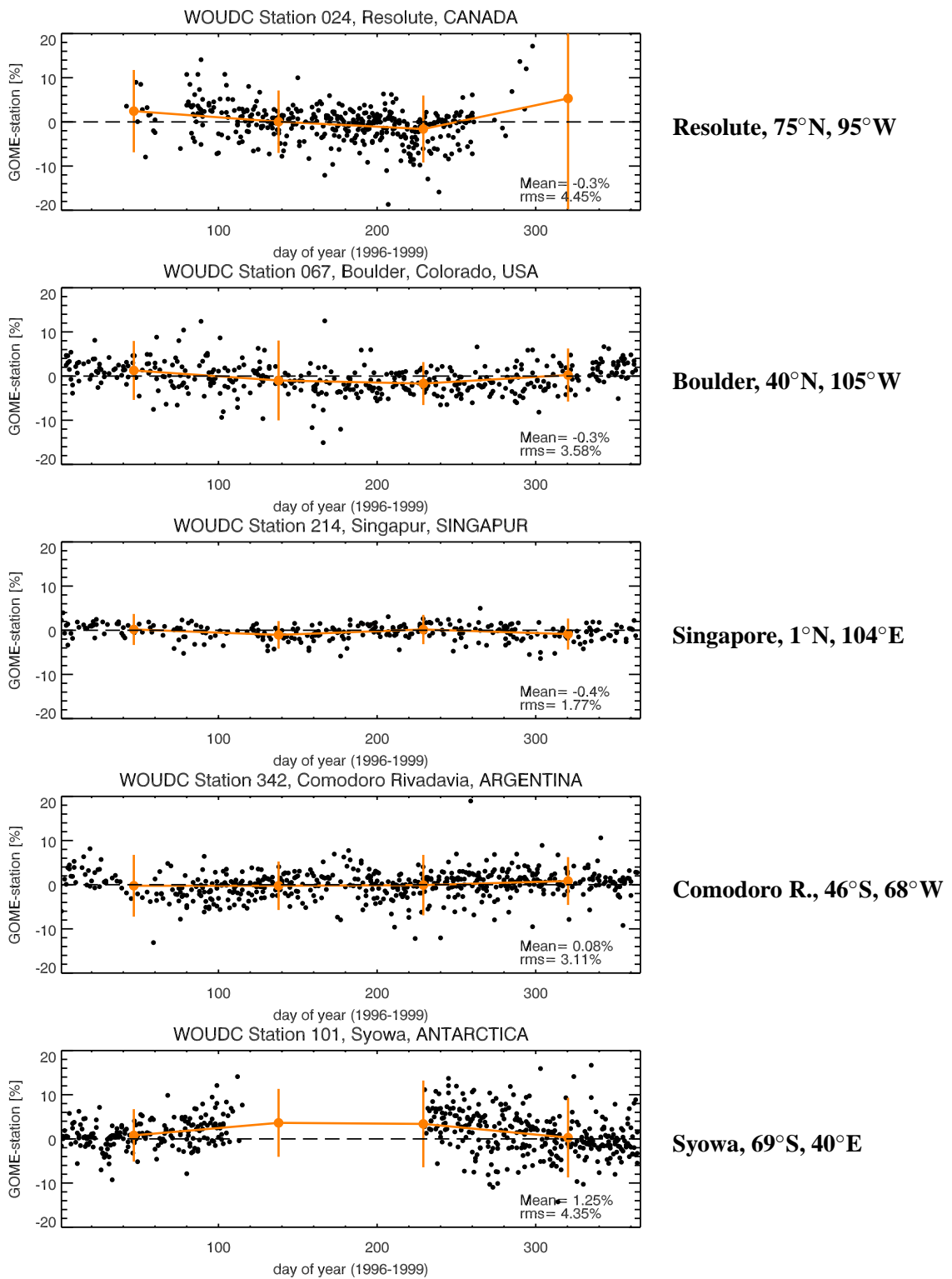


Figure 3.2: Same as Fig. 3.1, but shown as a function of season (day in year).

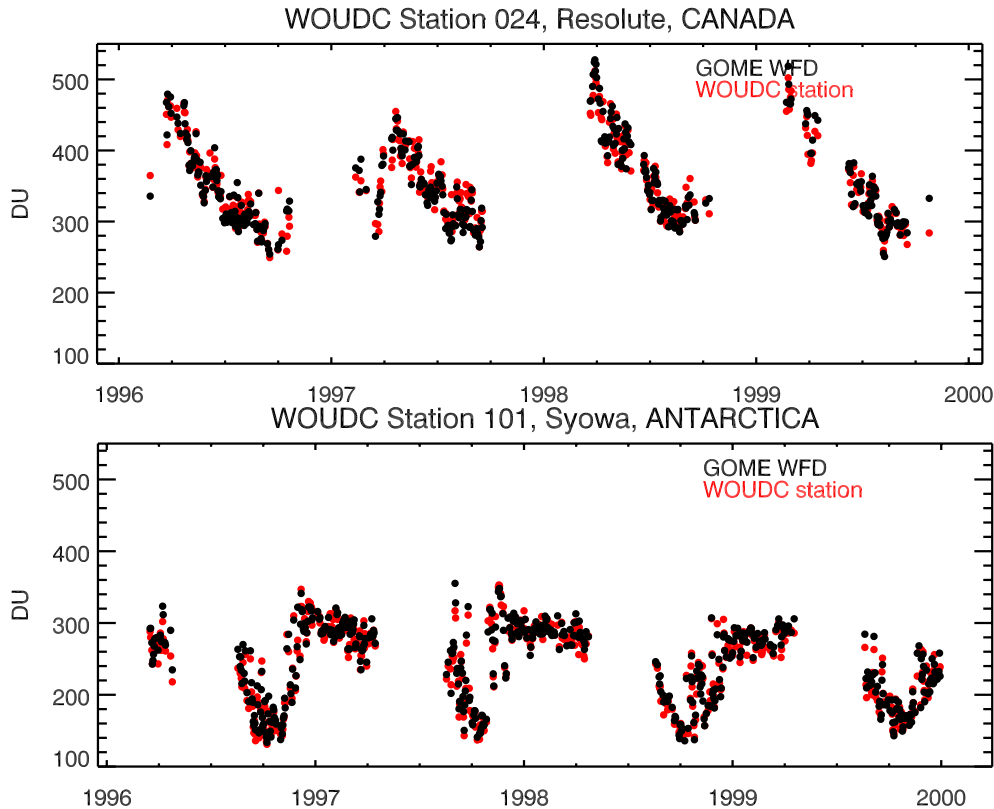


Figure 3.3: WF-DOAS V1.0 (WFD-HI) and Dobson ozone (WOUDC) time series from Resolute (75°N, top) and Syowa (69°S, bottom) in 1996–1999.

For mid-latitude station the scatter of the differences between WF-DOAS V1.0 and the WOUDC data are usually on the order of 3% (1σ) or better and increases to 4–5% at high latitudes. This agrees with the precision estimate of 3% (low- and mid-latitude) and 5% (polar region) as discussed in the ATBD. At some well maintained station time series the RMS can be as low as 2% if limited to AD pair direct-sun measurements or Brewer (see Hradec-Kralove and MOHp comparison in the previous section).

3.2 Statistical analysis

About 45 stations have been carefully selected for a statistical analysis in five latitude bands: polar regions (60°S–90°S, 60°N–90°N), mid-latitudes (30°S–60°S, 30°N–60°N) and tropics (–25°S–25°N). They are listed in Appendix A. Many more stations have been analyzed particularly in the northern hemisphere, but the selection was limited to 17 stations fairly evenly distributed in longitude direction. Hohenpeissenberg is contained in this list, but has not been included in the statistics. Other stations had inconsistent data, for instance biases of more than 5%, large jumps within a brief period, and those were excluded.

The GOME analysis was done twice, using mid- (WFD-MI) and high-latitude (WFD-HI) TOMS V7 ozone a-priori profile shapes, respectively. In the tropics low- (WFD-LO) and mid-latitude ozone profiles were selected. The data have been binned into three-month averages starting in spring 1996 and ending in fall 1999. In order to evaluate the spread of the various station data the 1σ RMS of the scatter for each three month period has been calculated and usually the 2σ range is shown in the plots (only for default WFD climatology). A plot summarizing the comparison between different analysis, GDP V3, WFD-HI, and WFD-MI with seventeen mid-latitude stations is shown in Fig. 3.4. The average annual bias is -0.4% for WFD-MI, the default analysis for this latitude band. A small seasonal variation of about $\pm 0.5\%$ can be seen, with maximum in winter and

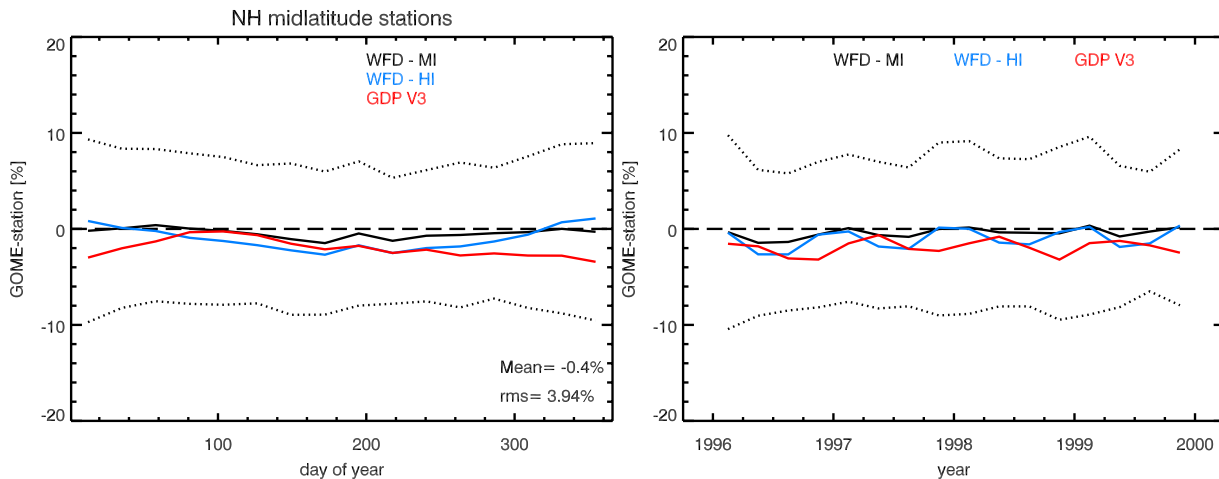


Figure 3.4: Average difference of WF-DOAS V1.0 and GDP V3.0 differences to seventeen NH mid-latitude WOUDC stations: 1996–1999. Left: annual course, right: all years. WFD-MI refers to mid-latitude a-priori ozone climatology and WFD-HI to high-latitude profiles. Black lines refer to the default retrieval (here WFD-MI) and 2σ RMS in differences.

minimum in summer statistically confirming the results from the individual station comparison. If the high-latitude profiles are used the seasonal variability doubles to $\pm 1\%$ with a lower annual bias. The GDP V3.0 shows a similar annual variability of $\pm 1\%$ with a bias of around -1% with respect to the station data. However, the maximum and minimum in the GDP difference are shifted towards spring (maximum) and fall (minimum).

By looking at individual mid-latitude stations, it can be noted that for some stations the seasonal variation is absent (e.g. Uccle, Belgium), while for other stations a weak seasonal cycle is observed with WF-DOAS. In order to see the effect on the statistics by selecting different stations, comparison has in one case been limited to eight European stations (Arosa, Lindenberg, Postdam, Hohenpeissenberg, Hradec-Kralove, Uccle, Camborne, and Oslo), while in a second selection fourteen Russian stations have been statistically analysed. Three of these stations are also included in the overall statistics of NH mid-latitude station validation (see Fig. 3.4 and Table A.1 in Appendix A). The Russian stations mainly use the so-called M-124 filter spectrometers to measure ozone (Gushchin *et al.*, 1985).

Figure 3.5 shows the statistics on the European and Russian stations. The difference to the Russian data show a pronounced seasonal cycle on the order of $\pm 3\%$ with highest differences in winter and minimum in summer. Almost no seasonal variation is observed in the mean difference to the European stations. The Russian M-124 spectrometers apparently suffers from stray light in winter similar to the Dobson instruments.

Looking at the SH mid-latitude differences as shown in Fig. 3.6 a similar pattern (now shifted by six month) observed with regard to GDP and WFD-HI can be concluded. However, the default WFD-MI differences show no significant annual cycle, similar to the European stations (Fig. 3.5). It may be due to the fewer stations involved in the comparison (six stations) that may mask a weak seasonal signal on the order of half percent as observed in the NH.

Figure 3.7 shows the results for the tropics. The bias due to different algorithms is fairly constant over the four year time span. The default WFD-LO analysis is about 0.8% higher than WOUDC, while WFD-MI nearly 0% and GDP -1% . Polar results are shown in Figs. 3.8 and 3.10 for both hemispheres. The southern hemispheric data show on average a difference of four percent with respect to ground-based data near the polar night period, in some cases can reach 10% like in Antarctic spring 1997. Over the annual cycle the average bias is about 1% . This comparison is difficult since solar elevation angles are low and large gradients near the polar vortex edge leads to the huge scatter in the RMS which can reach a 2σ value of 40% .

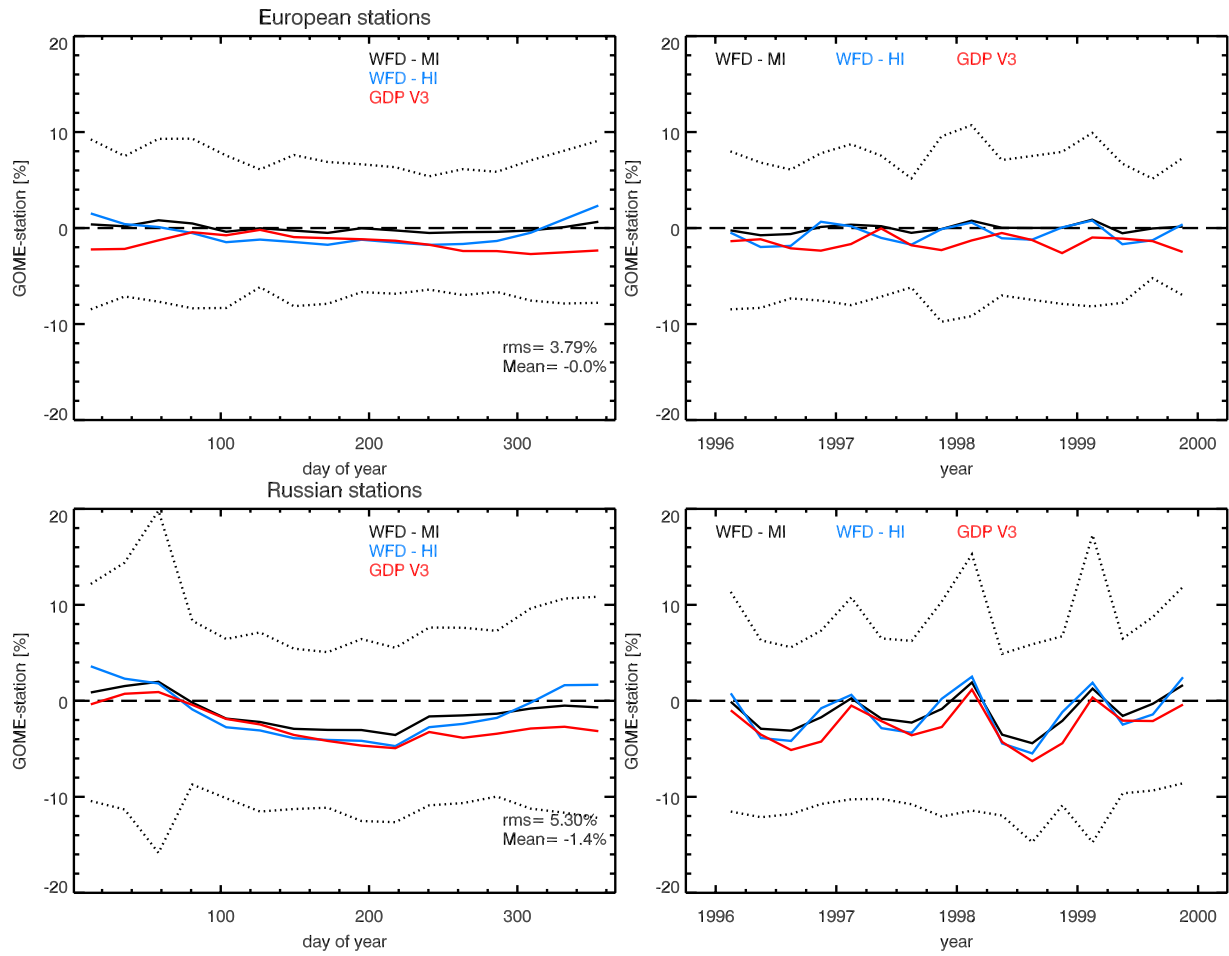


Figure 3.5: Same as Fig. 3.4, but for eight European stations (top) and fourteen Russian stations (bottom). see text for further details.

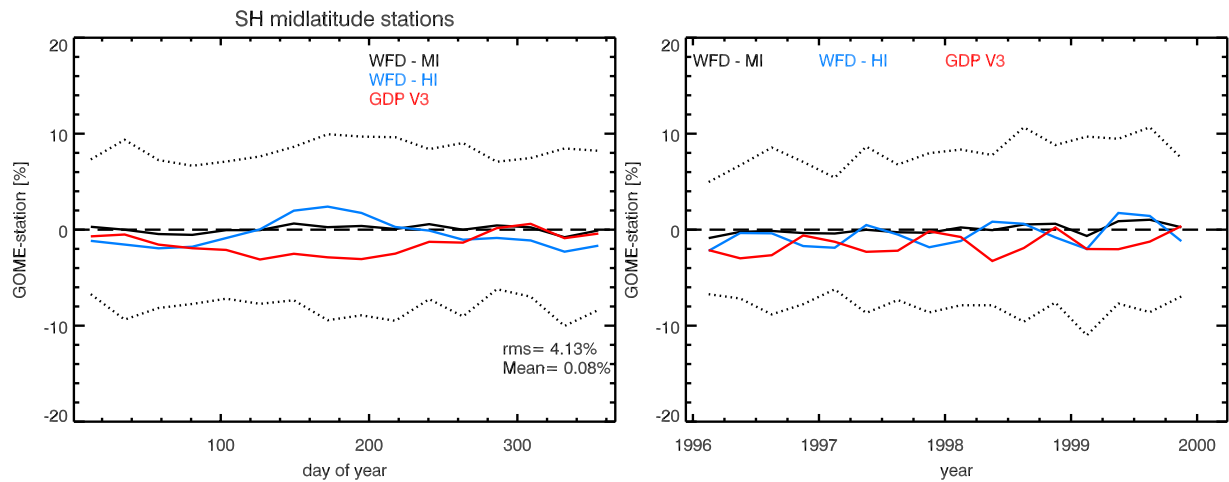


Figure 3.6: Same as Fig. 3.4, but for southern hemisphere mid-latitude stations (six stations).

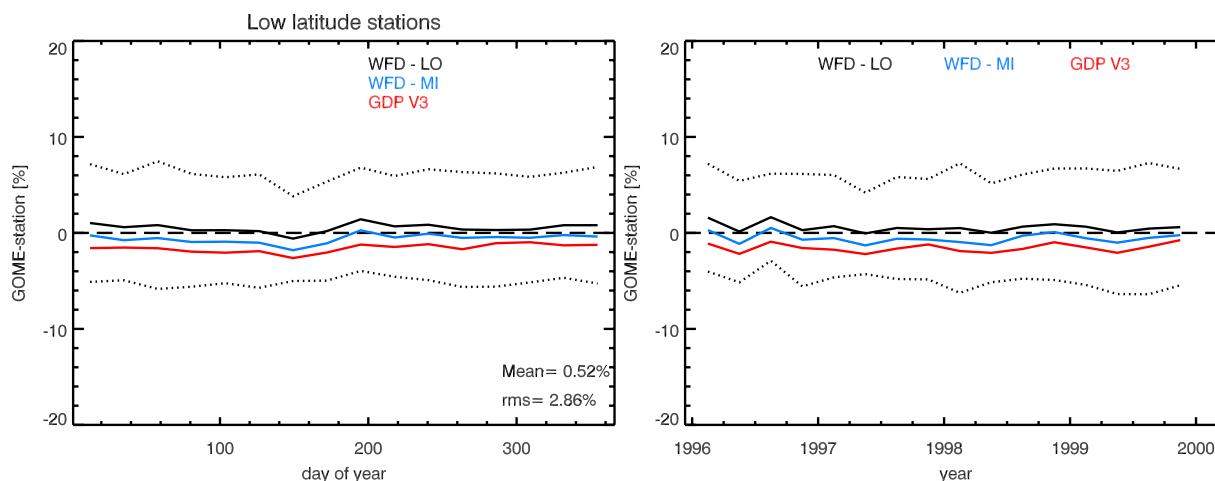


Figure 3.7: Same as Fig. 3.4, but for tropics. Default analysis is WFD-LO (black). Data from nine stations were analyzed.

If one plots the polar SH differences as a function of total ozone as shown in Fig. 3.9 it becomes evident that the largest error occurs at low total ozone below 150 DU with a bias up to 20% near 100 DU. One should note that the RMS at that values is almost $\pm 30\%$, so that in some cases GOME may be even lower than the station. Total ozone from two stations, Marambio and Arrival Heights, show strong in-and-out the vortex changes, while Halley Bay and Syowa (see Figs. 3.1 and 3.2) remain well inside the ozone hole for an extended period. In the latter cases, the bias gets relatively small ($<5\%$).

Similar arguments apply to the NH polar stations as shown in Fig. 3.10 but not as extreme as in the SH. The seasonal variation in the differences for both WF-DOAS and GDP is very similar to the one observed at mid-latitudes, but enlarged. It appears that in all GOME analyses the winter differences has increased from 1996 up to 1999. It is known that the NH polar ozone shows large interannual variability inside and outside of the polar vortex (Weber *et al.*, 2002, 2003, see for instance). The Arctic winter 1997/98 and 1998/99 have been rather warm stratospheric winters with high ozone beyond 500 DU (see also Fig. 3.3), while 1996/97 marked the end of a series of cold stratospheric Arctic winters in the mid-nineties with lower winter total ozone levels. It appears that at low solar elevation and higher total ozone the winter differences are closer to 5% (1998/99) and otherwise closer to +2 to +3%. The apparent trend seen in Fig. 3.10 may be therefore accidental. It also cannot be ruled out, that some of the station data may have drifted during that time.

It is instructive to look at a polar station that is usually outside the polar vortex region. The comparison with Barrow, Alaska, as shown in Fig. 3.11 shows the comparison between WFD-HI and Dobson and also shows the comparison with GDP V3. The seasonal pattern very much resembles that of mid-latitudes. WF-DOAS V1.0 has its maximum in fall/winter, while GDP V3.0 has its maximum shifted toward spring. Due to the lower solar elevation the variability from minimum to maximum is about $\pm 1\%$ for WFD and $\pm 3\%$ for GDP about twice as high as observed in mid-latitudes.

3.3 Ozone hole observation

Particular interest in total ozone monitoring is the development of the Antarctic ozone hole from year-to-year. In the WOUDC statistics four stations from Antarctica have been included for the SH polar stations. It was found that close to the polar night period GOME WF-DOAS V1 as well as GDP V3.0 can be up to 10% higher on average than ground based Dobson. However the variability of the differences is also very large, so that the differences observed may be also to a large extent depend on the station. In Fig. 3.12 the results from GOME

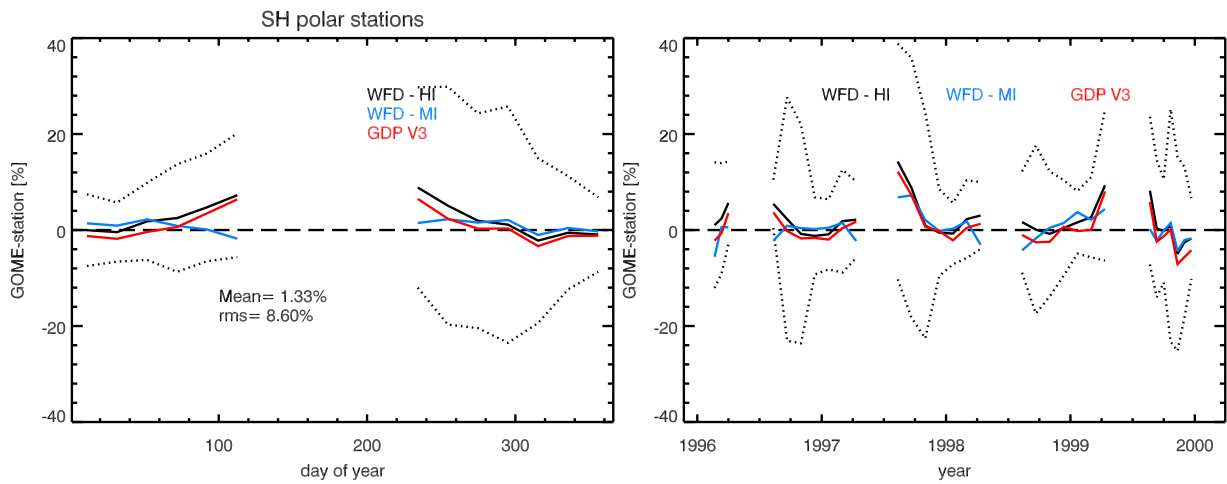


Figure 3.8: Same as Fig. 3.4, but for SH polar region. Four stations have been compared here.

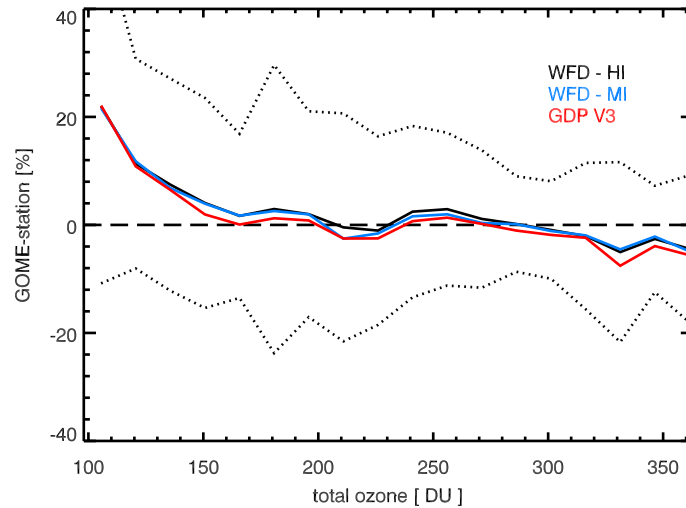


Figure 3.9: Same as Fig. 3.8, but differences are shown as a function of SH polar station total ozone.

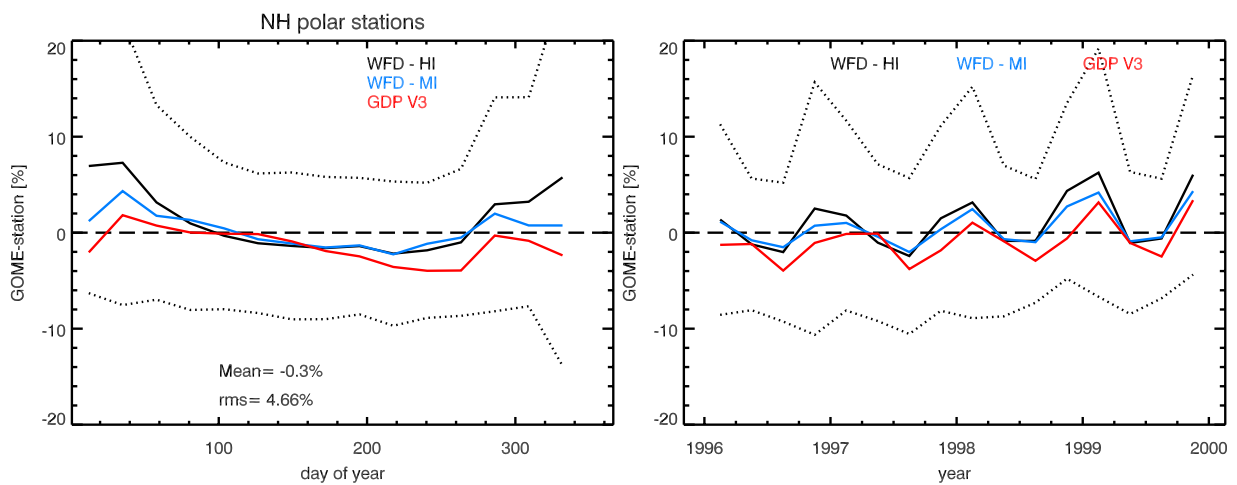


Figure 3.10: Same as Fig. 3.4, but for NH polar region. Five stations have been compared here.

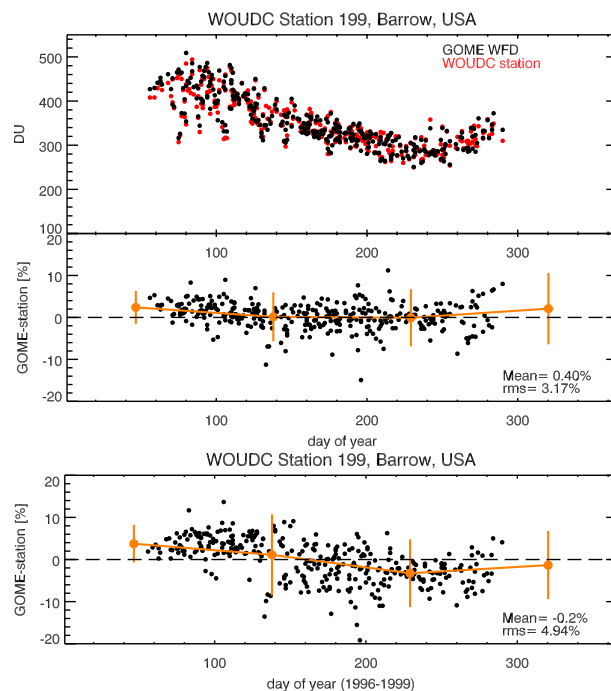


Figure 3.11: Comparison between WF-DOAS V1.0/GDP V3.0 with Barrow, Alaska (71° N), station data. Top: WF-DOAS and station data, Middle panel: Differences in percent, bottom panel: GDP V3.0 differences.

and Dobson comparison for each of the four Antarctic stations, Syowa, Halley Bay, Marambio, and Arrival Heights, are shown as a function of day of year covering the 1996–1999 period.

At each of the station the drop in total ozone can be observed in spring with minimum ozone reached near day 260. However, the ozone variability is quite large in Marimbo and Arrival Heights, that appear to move in and out of the polar vortex quite frequently. This most likely explains the large variability in the differences observed, when station and GOME may be at different locations with respect to vortex position despite being close in distance. Near the polar vortex edge ozone shows the largest gradients. All stations show enhanced variability during the ozone hole period, but it can be noticed that the Arrival Heights data show quite large variability with respect to GOME throughout the year. To a lesser extent this is also true for Marimbo. These two stations appear to be rather close to the vortex edge, while Syowa and Halley Bay remain for most days well inside the polar vortex.

In Figure 3.13 all GOME-station differences in percent are shown as a function of solar zenith angle and total ozone. The large scatter in the observed differences from Arrival Heights and Marimbo are clearly noticeable. The Halley Bay and Syowa differences show a slight upward trend of up to 5% near 90° solar zenith angle. Except for the lowest total ozone as observed at Halley Bay with values near 10% (below 140 DU) there appears only a weak dependence on total ozone. It should be noted that for GOME total ozone above 250 DU similar differences are observed as for the lowest ozone values below 140 DU. This may indicate that the apparent trend in Fig. 3.13 is related to the solar zenith angle dependency rather than due to total ozone. This is also consistent with larger differences between WF-DOAS V1.0 and Dobson observed in late fall well before the large scale ozone depletion starts. At low solar elevation the groundbased instruments suffer from increased stray light (underestimating total ozone, see earlier Discussion) and, in addition, GOME may suffer from lower signal-to-noise ratios since less photons reach the satellite borne spectrometer.

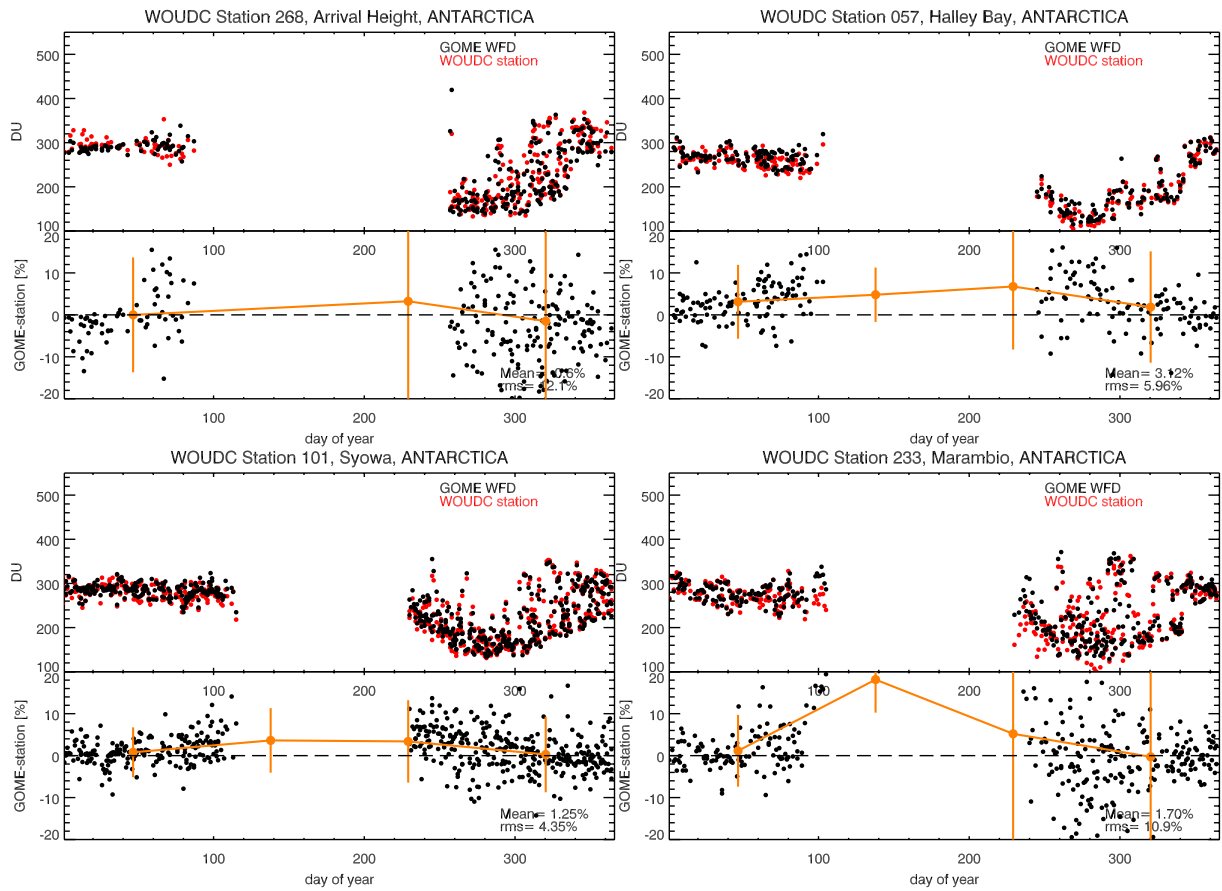


Figure 3.12: WF-DOAS V1 and Dobson total ozone as a function of day of year for four SH polar stations: Arrival Heights (78° S), Halley Bay (74° S), Syowa (69° S), and Marambio (64° S).

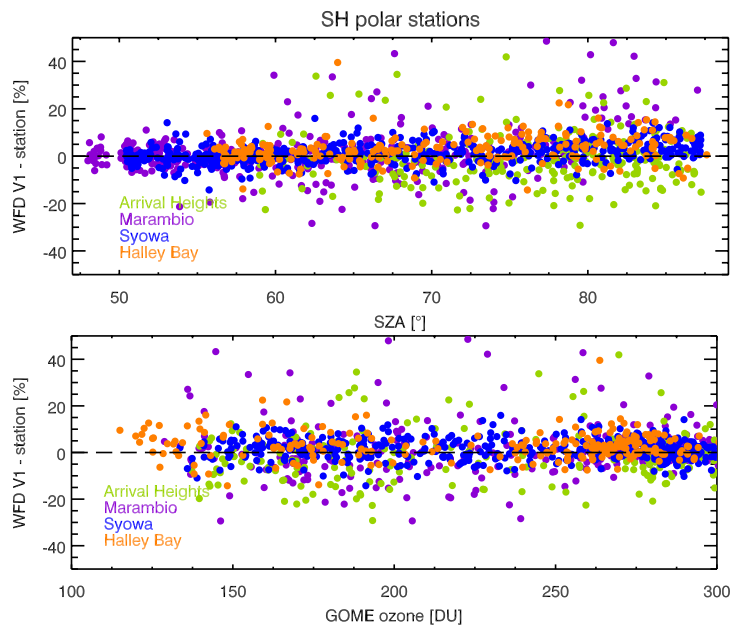


Figure 3.13: WF-DOAS V1 and Dobson total ozone as a function of solar zenith angle (top) and GOME total ozone (bottom) for four SH polar stations: Arrival Heights (78° S), Halley Bay (74° S), Syowa (69° S), and Marambio (64° S).

4 Summary and Conclusion

The new WF-DOAS algorithm has been extensively compared with globally distributed ground-based data, predominantly Dobson spectrophotometer data. In mid-latitudes it agrees on average to within half a percent with the WOUDC data. A small seasonal variation of about $\pm 0.5\%$ is noted, with a maximum in the differences in fall/winter and a minimum in spring/fall. At many mid-latitude stations, e.g. Lauder and Uccle, no seasonal variation is observed. GDP V3 clearly shows a larger annual variation ($\pm 1\%$) but the maximum in the differences is shifted towards spring (minimum in fall). This is a persistent pattern that has been observed in earlier GDP Version. The most recent GDP version has so far succeeded in decreasing that variability down to the 1.5% level. The seasonal pattern, when observed in SH, is generally shifted by six months. No variability is seen in the WF-DOAS in SH mid-latitude regions, but that may be accidental due to the lower number of stations available.

No major changes are observed with the new WF-DOAS in the tropics, a constant bias between WFD-DOAS (below +1%) and GDP (about -1%) with respect to the ground-based data throughout all years are observed.

In the polar region larger positive differences are observed with WF-DOAS at high solar zenith angles (up to 4%). If comparisons are made near the polar vortex edge errors can get quite large (up to 40%). If both GOME and the station are well inside the ozone hole it appears that the differences are below 5%. If one compares WF-DOAS at a northern high-latitude stations away from the European sector where the polar vortex mostly resides in NH winters, the seasonal pattern in WF-DOAS and GDP V3.0 is very similar to mid-latitudes stations.

The comparison with the Brewer instruments at Hradec-Kralove and Hohenpeissenberg has demonstrated excellent agreement with WF-DOAS. The maximum in the differences between GOME and Dobson and to a lesser extent with Brewer is related to the fixed ozone temperature used in the standard retrieval of the ground-based instruments. Brewer-Dobson differences can be as high as $\pm 2\%$ (generally on the order of 0.5%). This variability gets maximum at high latitudes due to lower solar elevation and the enhanced stray-light problem associated with it. The Fairbanks campaign TOMS3-F, where differences of up to 3-4% between Brewer and standard Dobson were measured in late winter, seem to support this conclusion (Staehelin *et al.*, 2003). The closer agreement of WF-DOAS with Brewer than simultaneous Dobson data confirm that the temperature shift weighting function appears appropriate to account for the ozone temperature variation. This has been confirmed by comparison with ozone temperature corrected ground-based data (Vanicek *et al.*, 2003).

Overall it can be concluded that the accuracy of the WF-DOAS V1.0 results are now within the uncertainty of the ground-based measurements.

The TOMS V7 climatology (Wellemeyer *et al.*, 1997) seems to work well in WF-DOAS V1.0. Using a false climate zone (mid-latitude profiles in polar region, for instance) seems still to provide very reasonable results but make generally the comparison to ground-based data slightly worse and increases the seasonal variability somewhat. Particularly, the mid-latitude TOMS V7 ozone profiles can be globally applied in the retrieval except in polar regions at high solar zenith angles where differences become more distinct. The largest differences are also to be expected at moderate low ozone 220-280 DU when two types of profile shapes produce the same ozone column density, namely a weakly ozone depleted ozone hole profile and a high tropopause profile. Both can be observed frequently at mid- to high latitudes.

The very good agreement with ground based instruments are proof that several issues that has been newly introduced in WF-DOAS V1.0 have drastically improved total ozone retrieval: 1) ozone filling-in as part of the Ring effect, 2) the introduction of an effective scene height from cloud information and 3) derivation of an effective scene albedo from the GOME spectral measurements. These changes are, however, not specific to the type of algorithm that has been used here but can be potentially applied to other retrieval schemes as well. The WF-DOAS theoretical approach is a straight forward formulation of the DOAS inversion and is applicable in a more general way than the standard DOAS approach that uses airmass factors to correct for the slant path

geometry.

Acknowledgement

We thank Ulf Köhler and Hans Claude, MOHp Heissenberg, for providing us with their station data (Brewer and Dobson) and for their insights into the ground-based measurements. We also thank Bob Evans, NOAA, for providing us data from Lauder and he kindly informed us on the accuracy of the Dobson spectrophotometers. We thank Rene Stuebi, Swiss Meteo, who put for us together Brewer and Dobson data from Arosa.

References

- BASHER, R.E. 1995. *Survey of WMO-sponsored Dobson spectrophotometer intercomparisons*. Tech. rept. World Meteorological Organization. WMO Global Ozone Research and Monitoring Project Report 19.
- BRAMSTEDT, K., GLEASON, J., LOYOLA, D., THOMAS, W., BRACHER, A., WEBER, M., and BURROWS, J. P. 2003. Comparison of total ozone from the satellite instruments gome and toms with measurements from the dobson network 1996–2000. *Atmos. Chem. Phys.*, **3**, 1409–1419.
- BURROWS, J. P., DEHN, A., DETERS, B., HIMMELMANN, S., RICHTER, A., VOIGT, S., and ORPHAL, J. 1998. Atmospheric remote-sensing reference data from GOME: Part 1. Temperature-dependent absorption cross sections of NO₂ in the 231–794 nm range. *J. Quant. Spectrosc. Rad. Transfer*, **60**, 1025–1031.
- BURROWS, J. P., RICHTER, A., DEHN, A., DETERS, B., HIMMELMANN, S., VOIGT, S., and ORPHAL, J. 1999. Atmospheric remote-sensing reference data from GOME: Part 2. Temperature-dependent absorption cross sections of O₃ in the 231–794 nm range. *J. Quant. Spectrosc. Rad. Transfer*, **61**, 509–517.
- CHANCE, K., and SPURR, R. J. D. 1997. Ring effect studies: Rayleigh scattering, including molecular parameters for rotational Raman scattering and the Fraunhofer spectrum. *Appl. Opt.*, **36**, 5224 – 5230.
- DOBSON, G.M.B. 1931. A photo-electric spectrometer for measuring the amount of atmospheric ozone. *Proc. Phys. Soc.*, 324–339.
- DOBSON, G.M.B. 1968. Forty year's research on atmospheric ozone at Oxford: a history. *Appl. Opt.*, 387–405.
- GDP V3 VALREPORT. 2002. *ERS-2 GOME GDP 3.0 implementation and delta validation report*. Technical Note ERSE-DTEX-EOAD-TN-02-0006, Issue 1.0, November 2002, ed. J.–C. Lambert, see also: http://earth.esrin.esa.it/pub/ESA_DOC/GOME/gdp3/gdp3.htm.
- GOME LVL2. 2000. GOME level 1 to 2 algorithms descriptions. *Tech. Rep. ER-TN-DLR-GO-0025, Issue 2B*. prepared by R. Spurr and W. Thomas, <http://atmos.af.op.dlr.de/cgi-bin/home.cgi?page=projdocs>.
- GRASS, R.D., KOMHYR, W.D., KOENIG, G.L., and EVANS, R.D. 1994. Results of international Dobson spectrophotometer calibrations at Arosa, Switzerland, 1990. *Pages 266–270 of: HUDSON, R.D. (ed), Ozone in the Stratosphere and Troposphere, Part 1, NASA Conference Publication 3266, Greenbelt, MD, USA*.
- GUSHCHIN, G.P., SOKOLENKO, S.A., and KOVALYOV, V.A. 1985. Total-ozone measuring instruments used at the USSR station network. *Pages 543–546 of: ZEREFOS, C.S., and GHAZI, A. (eds), Atmospheric ozone* Reidel, Dordrecht, for Commission of the European Communities.
- HARE, E., and FIOLETOV, V. 1998. An examination of the total ozone data in the World Ozone and Ultraviolet Radiation Data Center. *Pages 45–48 of: BOJKOV, R., and VISCONTI, G. (eds), Atmospheric ozone - proc. 18th quadrennial ozone symposium, l'aquila, italy*.
- HOOGEN, R., ROZANOV, V. V., and BURROWS, J. P. 1999. Ozone profiles from GOME satellite data: Algorithm description and first validation. *J. Geophys. Res.*, **104**, 8263–8280.
- KERR, J.B., MCELROY, C.T., WARDLE, D.I., OLAFSON, R.A., and EVANS, W.P.J. 1985. The automated Brewer spectrophotometer. *Pages 543–546 of: Atmospheric Ozone*. C.S. Zerefos and A. Ghazi.
- KERR, J.B., ASBRIDGE, I.A., and EVANS, W.F.J. 1988. Intercomparison of total ozone measured by the Brewer and Dobson spectrophotometers at toronto. *J. Geophys. Res.*, **93**, 11129–11140.

- KOELEMEIJER, R.B.A., STAMMES, P., HOVENIER, J.W., and DE HAAN, J.F. 2001. A fast method for retrieval of cloud parameters using oxygen A-band measurements from the Global Ozone Monitoring Experiment. *J. Geophys. Res.*, **106**, 3475–3496.
- KOMHYR, W.D., MATEER, C.L., and HUDSON, R.D. 1993. Effective Bass-Paur 1985 ozone absorption coefficients for use with Dobson ozone spectrophotometers. *J. Geophys. Res.*, **98**, 20451–20465.
- KURUCZ, R.L., FURENLID, I., BRAULT, J., and TESTERMAN, L. 1984. *Solar flux atlas from 296 nm to 1300 nm*. National Solar Observvatory, Sunspot, New Mexico.
- LAMBERT, J.C., VAN ROOZENDAEL, M., DE MAZIERE, M., SIMON, P.C., POMMERAU, J.-P., GOUTAIL, F., SARKISSIAN, A., and GLEASON, J.F. 1999. Investigation of pole-to-pole performances of space-borne atmospheric sensors with ground-based networks. *J. Atmos. Sci.*, **56**, 176–XXX.
- LAMBERT, J.C. ,*et al.* 1995. Combined characterisation of GOME and TOMS total ozone measurements from space using ground-based observations from NDSC. *Adv. Space Res.*, **35**, 445–451.
- STAEHELIN, J., KERR, J., EVANS, R., and VANICEK, K. 2003. *Comparison of total ozone measurements of Dobson and Brewer spectrophotometers and recommended transfer functions*. Tech. rept. World Meteorological Organization Global Atmosphere Watch (WMO-GAW) Report 149.
- STAEHELIN, J., *et al.* 1998. Total ozone series of Arosa (Switzerland). Homogenization and data comparison. *J. Geophys. Res.*, **103**, 5827–5841.
- TANZI, C.P., SNEL, R., HASEKAMP, O., and ABEN, I. 2001. Degradation of UV earth albedo observations by GOME. In: *ERS-ENVISAT Symposium, Gothenburg, 16-20 October 2000*. ESA Special Publication SP-461 (CD-ROM).
- VANICEK, K. 1998. Differences between Dobson and Brewer observations of total ozone at Hradec-Kralove. *Pages 81–84 of: BOJKOV, R.D., and VISCONTI, G. (eds), Atmospheric Ozone, Proc. Quadr. Ozone Symp.* Edigrafital S.p.A.-S.Atto (TE).
- VANICEK, K., STANEK, M., and DUBROVSKY, M. 2003. *Evaluation of Dobson and Brewer total ozone observations from Hradec Kralove Czech Republic, 1961–2002*. Tech. rept. Czech Hydrometeorological Institute. EU Project CANDIDOZ EVK2-2001-00024, Working Group WG-1.
- WAUGH, D.W. *et al.* 1997. Mixing of polar vortex air into middle latitudes as revealed by tracer-tracer scatterplots. *J. Geophys. Res.*, **102**, 13119–1313.
- WEBER, M., EICHMANN, K.-U., WITTRUCK, F., BRAMSTEDT, K., HILD, L., RICHTER, A., BURROWS, J.P., and MÜLLER, R. 2002. The cold arctic winter 1995/96 as observed by the Global Ozone Monitoring Experiment GOME and HALOE: Tropospheric wave activity and chemical ozone loss. *Quart. J. Roy. Meteorol. Soc.*, 1293–1319.
- WEBER, M., DHOMSE, S., WITTRUCK, F., RICHTER, A., SINNHUBER, B.-M., and BURROWS, J.P. 2003. Dynamical control of NH and SH winter/spring total ozone from GOME observations in 1995-2002. *Geophys. Res. Lett.*, **30**, 1853–1854. doi:10.1029/2002GL016799.
- WELLEMAYER, C. G., TAYLOR, S. L., SEFTOR, C. J., MCPETERS, R. D., and BHARTIA, P. K. 1997. A correction for the Total Ozone Mapping Spectrometer profile shape errors at high latitude. *J. Geophys. Res.*, **102**, 9029–9038.

Appendix

A List of stations from the WOUDC data base

In Table A.1 all stations that have been used to validate GOME WF-DOAS V1.0 are listed. These stations (45 stations) have been used in an earlier study to validate GOME GDP V2.7 total ozone (Bramstedt *et al.*, 2003). The ground based data can be obtained from the WOUDC web-page <http://www.woudc.org> (Hare and Fioletov, 1998).

Table A.1. List of WOUDC station data used in this validation report.

WOUDC Station No.	Latitude	Longitude	Altitude [m]	Location
024	74.72° N	94.98° W	65	Resolute, Canada
199	71.32° N	156.6° W	11	Barrow/Alaska, USA
105	64.82° N	147.87° W	138	Fairbanks, USA
051	64.13° N	21.9° W	75	Reykjavik, Iceland
123	62.08° N	129.75° E	98	Yakutsk, Russia
043	60.13° N	1.18° W	95	Lerwick, UK
077	58.75° N	94.07° W	35	Churchill, Canada
143	56.00° N	92.88° E	137	Krasnoyarsk, Russia
021	53.55° N	114.10° W	766	Edmonton/Stony Plain, Canada
076	53.32° N	160.38° W	44	Goose Bay, Canada
130	52.97° N	158.75° E	78	Petropavlovsk, Russia
174	52.22° N	14.12° E	112	Lindenberg, Germany
053	50.80° N	4.35° E	100	Uccle/Brussels, Belgium
036	50.22° N	5.32° W	88	Camborne, UK
099	47.80° N	11.02° E	975	Hohenpeissenberg, Germany
277	47.73° N	42.25° E	64	Cimljansk, Russia
020	46.87° N	68.02° W	192	Caribou, USA
119	46.48° N	30.63° E	42	Odessa, Ukraine
065	43.78° N	79.47° W	198	Toronto, Canada
012	43.05° N	141.33° E	19	Sapporo, Japan
067	40.02° N	105.25° W	1390	Boulder, USA
208	39.77° N	117.00° E	80	Shiangher, China
293	39.45° N	22.48° E	110	Athens, Greece
107	37.93° N	75.48° W	13	Wallops Island, USA
158	33.57° N	7.67° W	55	Casablanca, Morocco
031	19.53° N	155.57° W	3420	Mauna Loa/Hawaii, USA
187	18.53° N	73.85° E	559	Poona, India
218	14.63° N	121.83° E	61	Manila, Philippines
214	1.33° N	103.88° E	14	Singapore, Singapore
175	1.27° S	36.8° E	1745	Nairobi, Kenia
219	5.84° S	35.21° W	32	Natal, Brazil
084	12.42° S	130.88° E	31	Darwin, Australia
191	14.25° S	170.56° W	82	Samoa, American Samoa
200	22.68° S	45.00° W	573	Cachoeira Paulista, Brazil
027	27.42° S	153.12° E	18	Brisbane, Australia
343	31.38° S	57.97° W	31	Salto, Uruguay
091	34.58° S	58.48° W	25	Buenos Aires, Argentina
253	37.80° S	144.97° E	125	Melbourne, Australia
256	45.06° S	169.70° E	370	Lauder, Newzealand
342	45.78° S	67.5° W	43	Comodoro Rivadavia, Argentina
339	54.85° S	68.31° W	7	Ushuaia, Argentina
233	64.23° S	56.72° W	196	Marambio, Antarctica
101	69.00° S	39.58° E	21	Syowa, Japan
057	73.51° S	26.73° W	31	Halley Bay, UK
268	77.83° S	166.68° E	250	Arrival Heights, Antarctica

B Summary plots for GOME-WOUDC comparison in various regions

In the following all plots summarising the comparison between GOME (WF-DOAS V1.0 and GDP V3.0) and the ground-based data from WOUDC for each climate zone are shown. For each region, NH polar, NH mid-latitudes, tropics, SH mid-latitudes the following dependencies of the satellite-ground-based differences are shown (in order): dependence with respect to day of year, as a function of year, as a function of solar zenith angle, as a function of total ozone, and as a function of the added ghost vertical column. All the stations contributing to the statistics in each region are summarized in Appendix A. In each region two analysis have been performed, by using the default TOMS V7 climatology and the climatology of an adjacent region, i.e. high latitude (default) and mid-latitude climatology for polar region, mid-latitude (default) and high-latitude for mid-latitude stations in both hemispheres, and low-latitude (default) and mid-latitude for tropics. The used climatologies are indicated by HI, MI, LO and default is always plotted in black. Blue indicates the other climatological zone used in the retrieval, while the red line shows the GDP V3.0 results.

B.1 Northern hemisphere polar region, 60°N–90°N

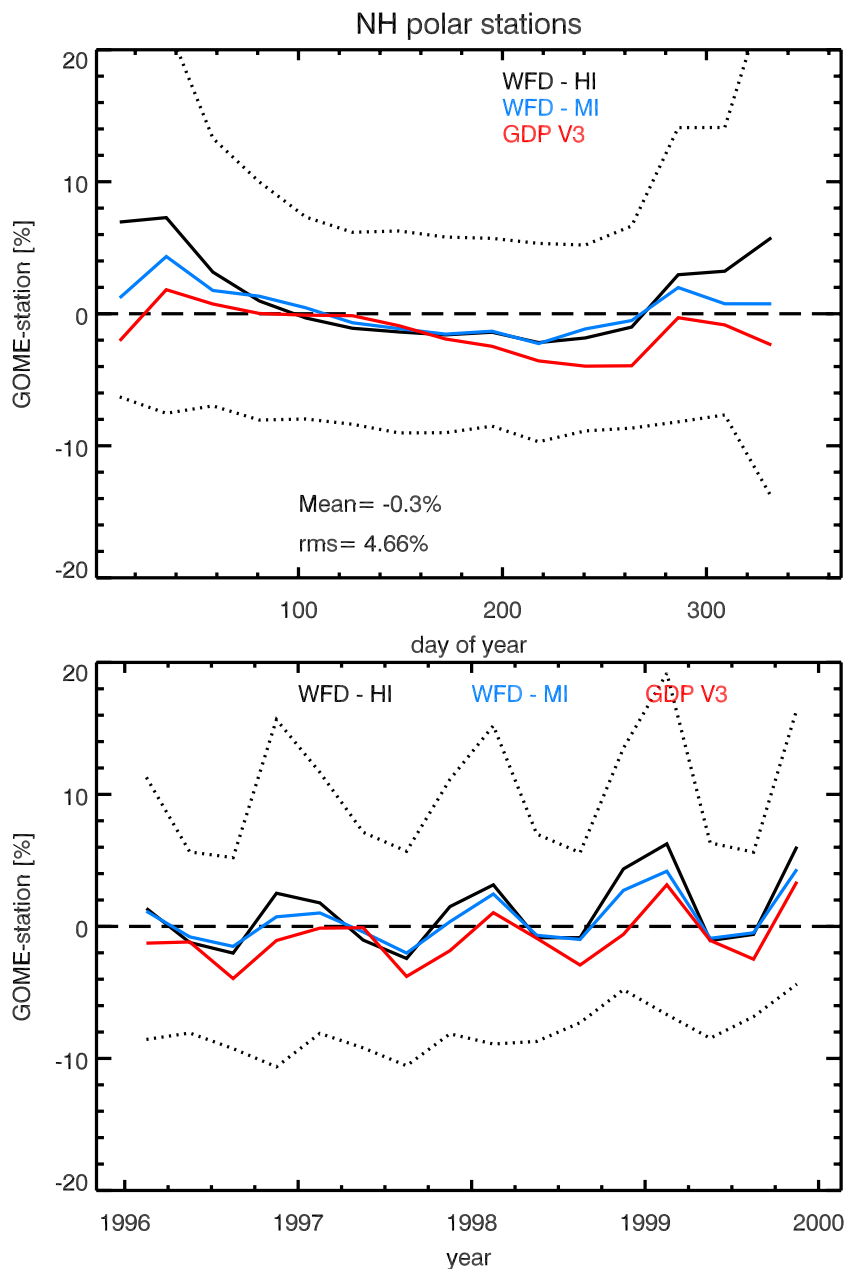


Figure B.1: Statistics on NH polar stations (six stations). Top: as function of day in year. Bottom: as a time series from 1996 to 1999. The lines mark seasonal averages (three month) and the dotted lines are the 2σ RMS in the observed differences (WF-DOAS with default TOMS V7 climatology).

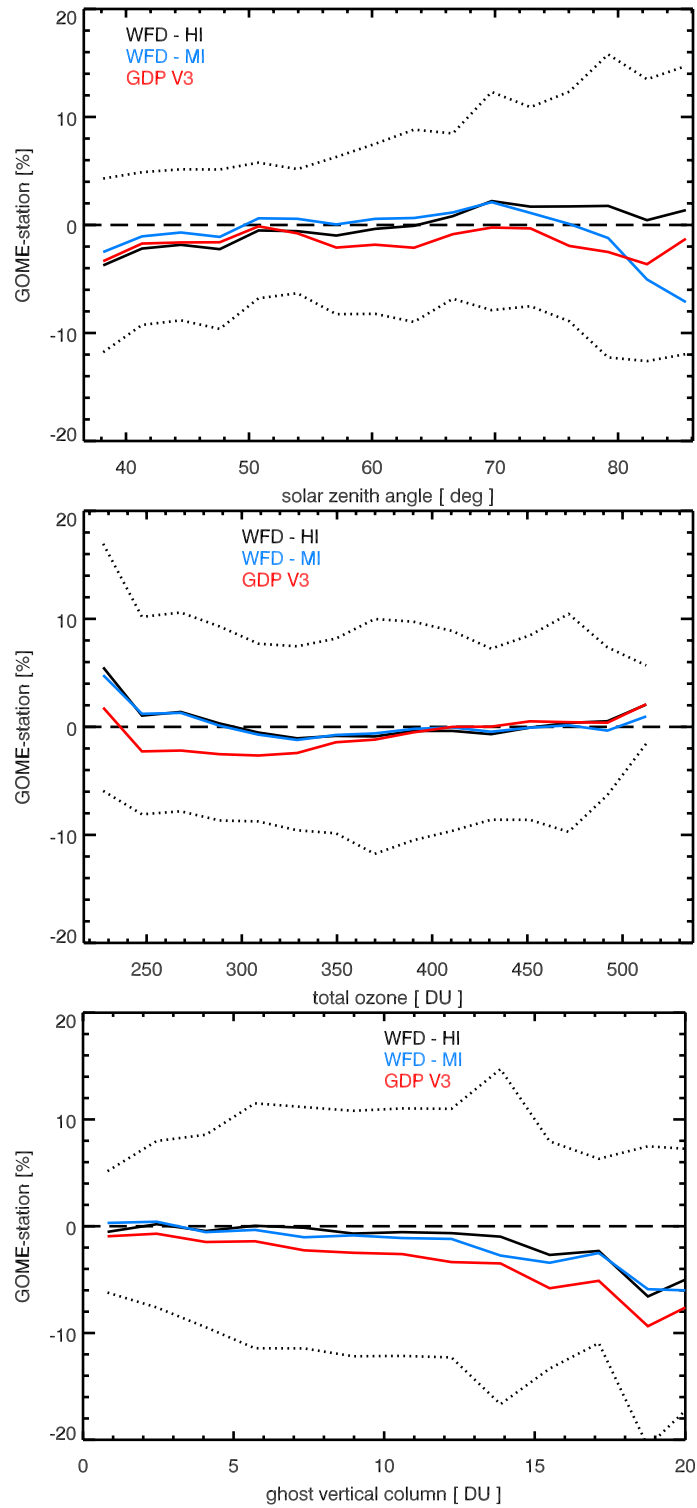


Figure B.2: Statistics on NH polar stations (six stations). Top: as a function of GOME solar zenith angle. Middle: as a function of total ozone. Bottom as a function of the ghost vertical column.

B.2 Northern hemisphere mid-latitude, 25°N–60°N

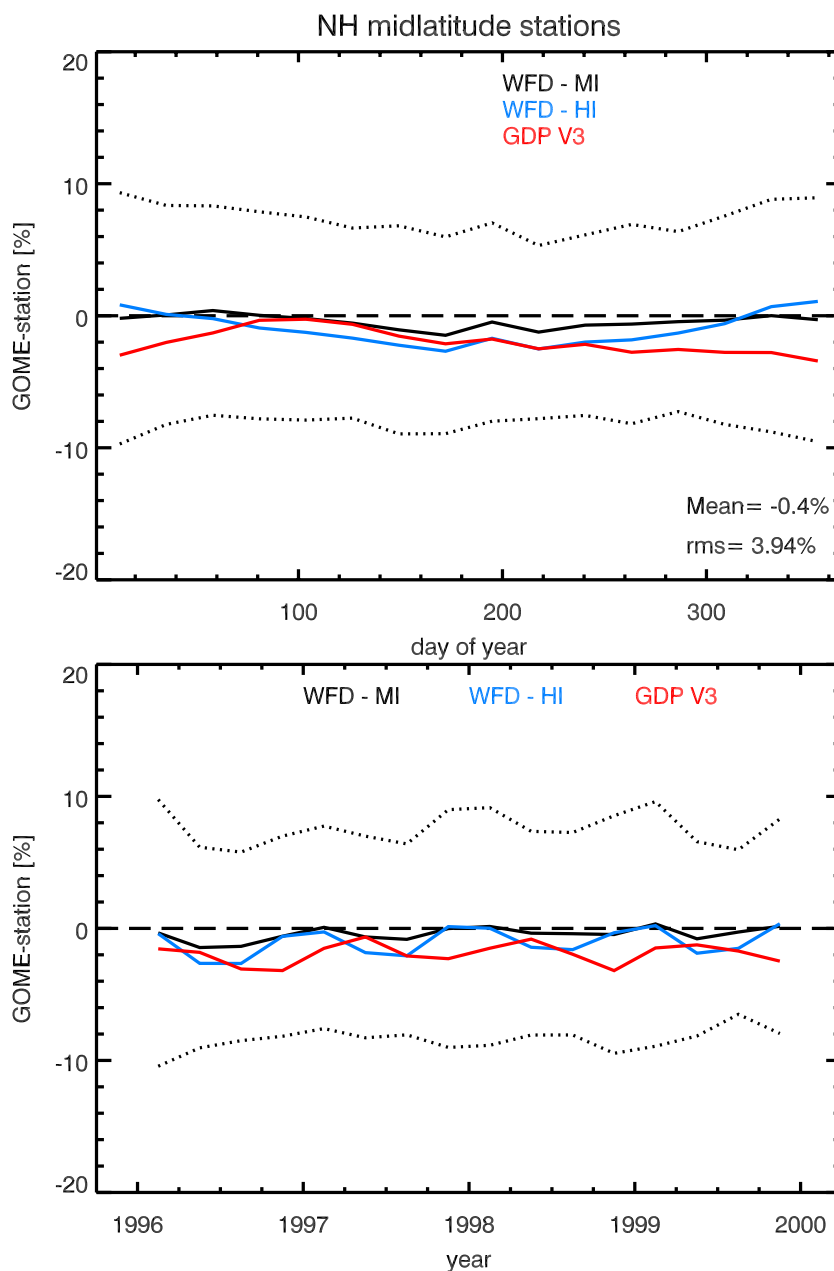


Figure B.3: Statistics on NH mid-latitude stations (seventeen stations). Top: as function of day in year. Bottom: as a time series from 1996 to 1999. The lines mark seasonal averages (three month) and the dotted lines are the 2σ RMS in the observed differences (WF-DOAS with default TOMS V7 climatology).

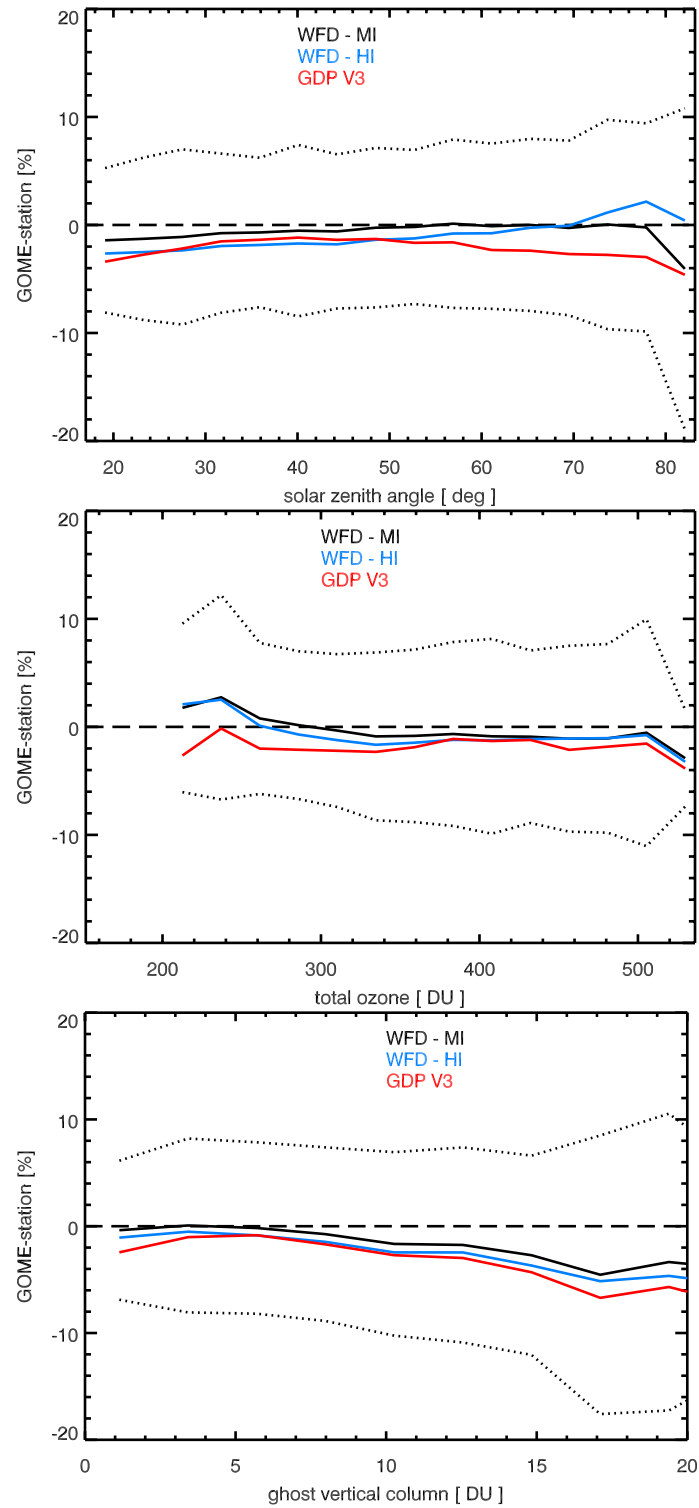


Figure B.4: Statistics on NH mid-latitude stations (seventeen stations). Top: as a function of GOME solar zenith angle. Middle: as a function of total ozone. Bottom as a function of the ghost vertical column.

B.3 Tropics, 25°S–25 °N

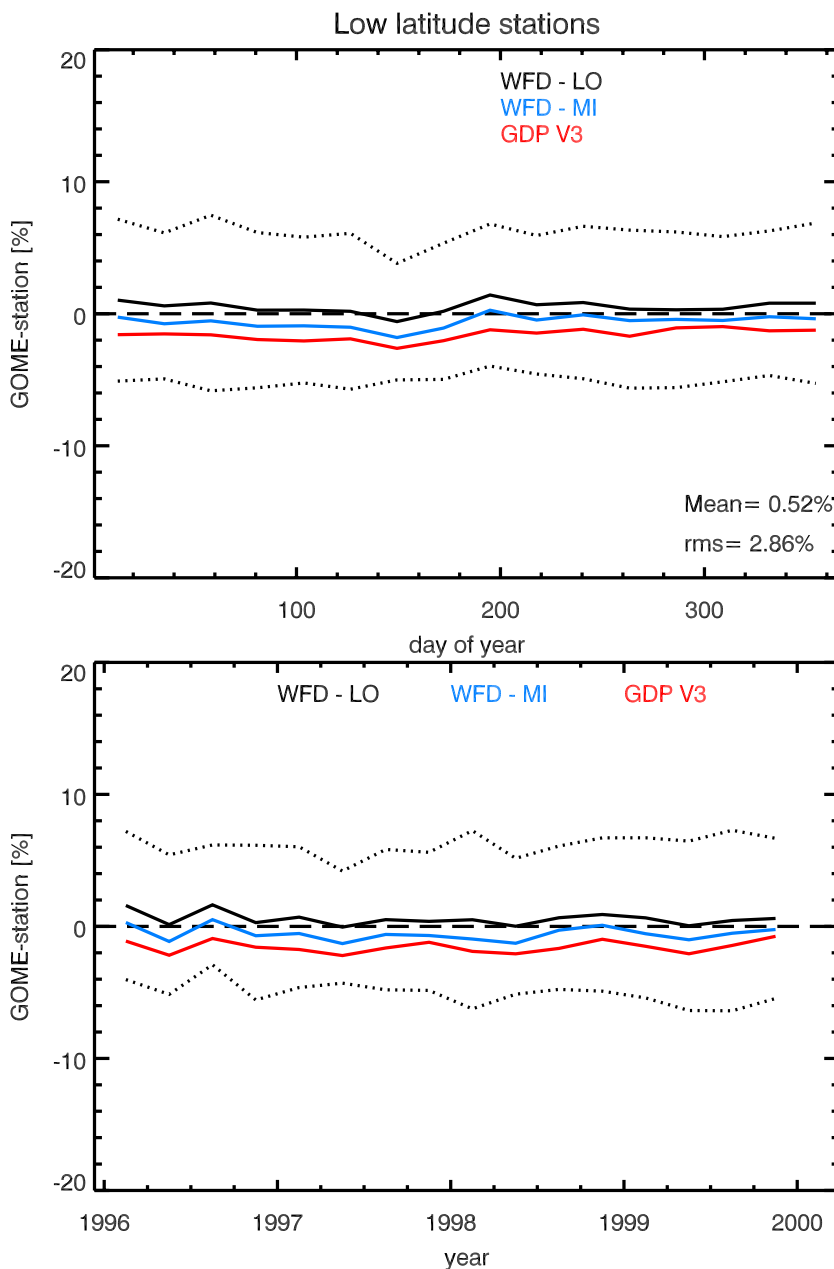


Figure B.5: Statistics on tropical stations (nine stations). Top: as function of day in year. Bottom: as a time series from 1996 to 1999. The lines mark seasonal averages (three month) and the dotted lines are the 2σ RMS in the observed differences (WF-DOAS with default TOMS V7 climatology).

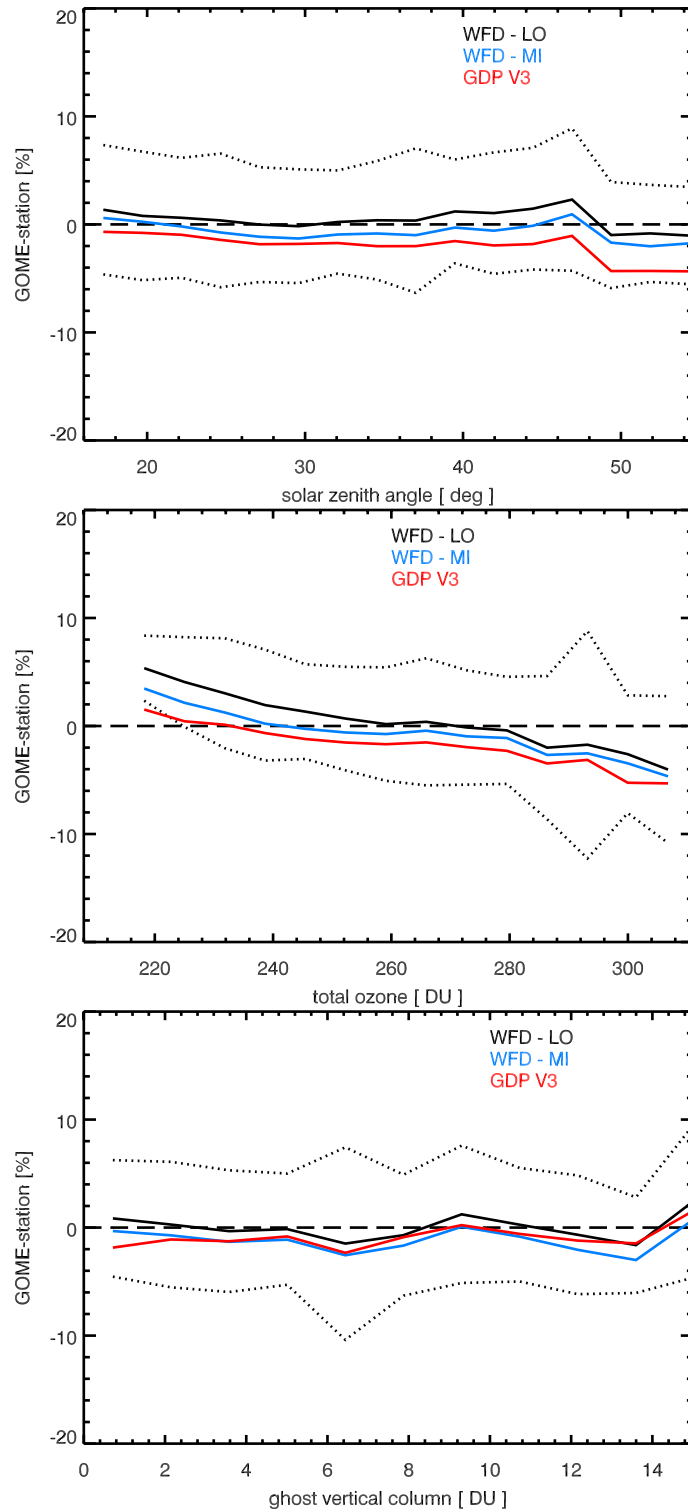


Figure B.6: Statistics on tropical stations (nine stations). Top: as a function of GOME solar zenith angle. Middle: as a function of total ozone. Bottom as a function of the ghost vertical column.

B.4 Southern hemisphere mid-latitude, 25°S–60°S

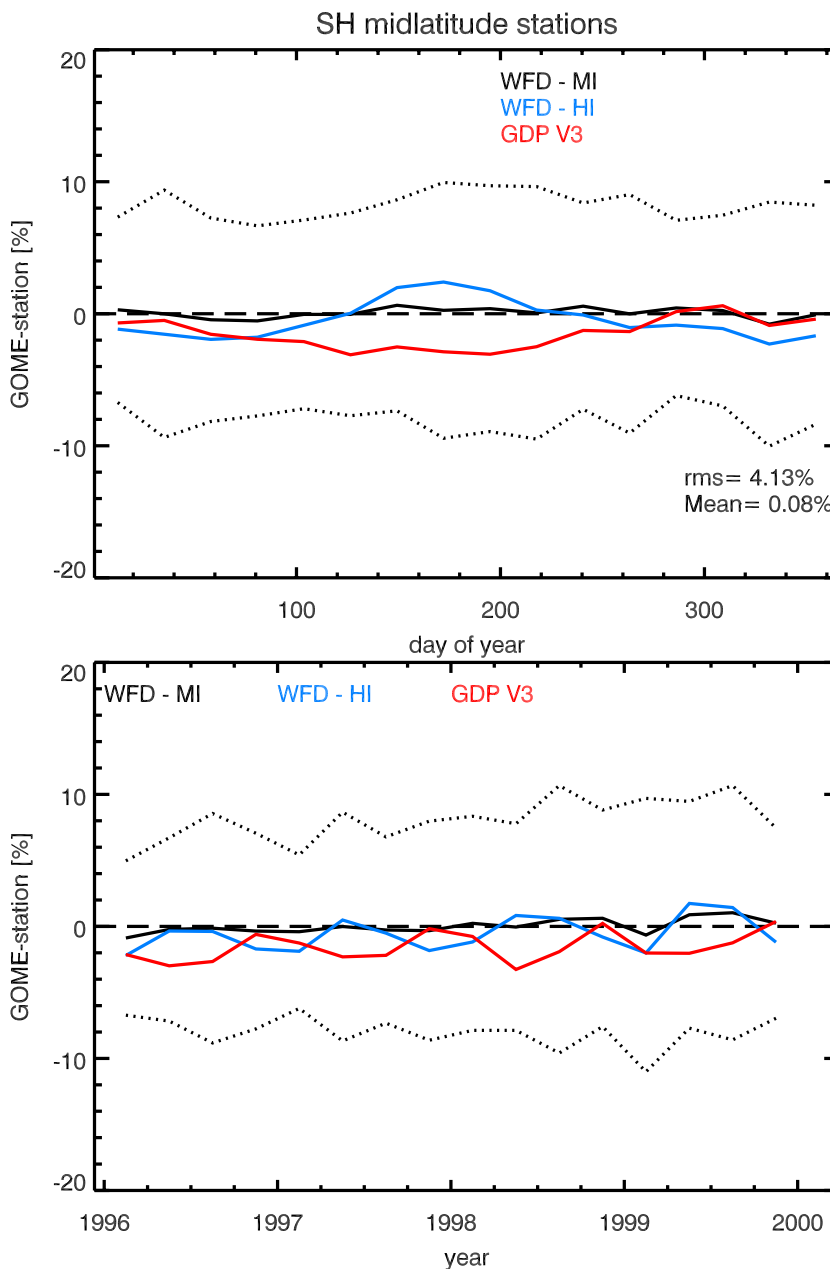


Figure B.7: Statistics on SH mid-latitude stations (six stations without Lauder). Top: as function of day in year. Bottom: as a time series from 1996 to 1999. The lines mark seasonal averages (three month) and the dotted lines are the 2σ RMS in the observed differences (WF-DOAS with default TOMS V7 climatology).

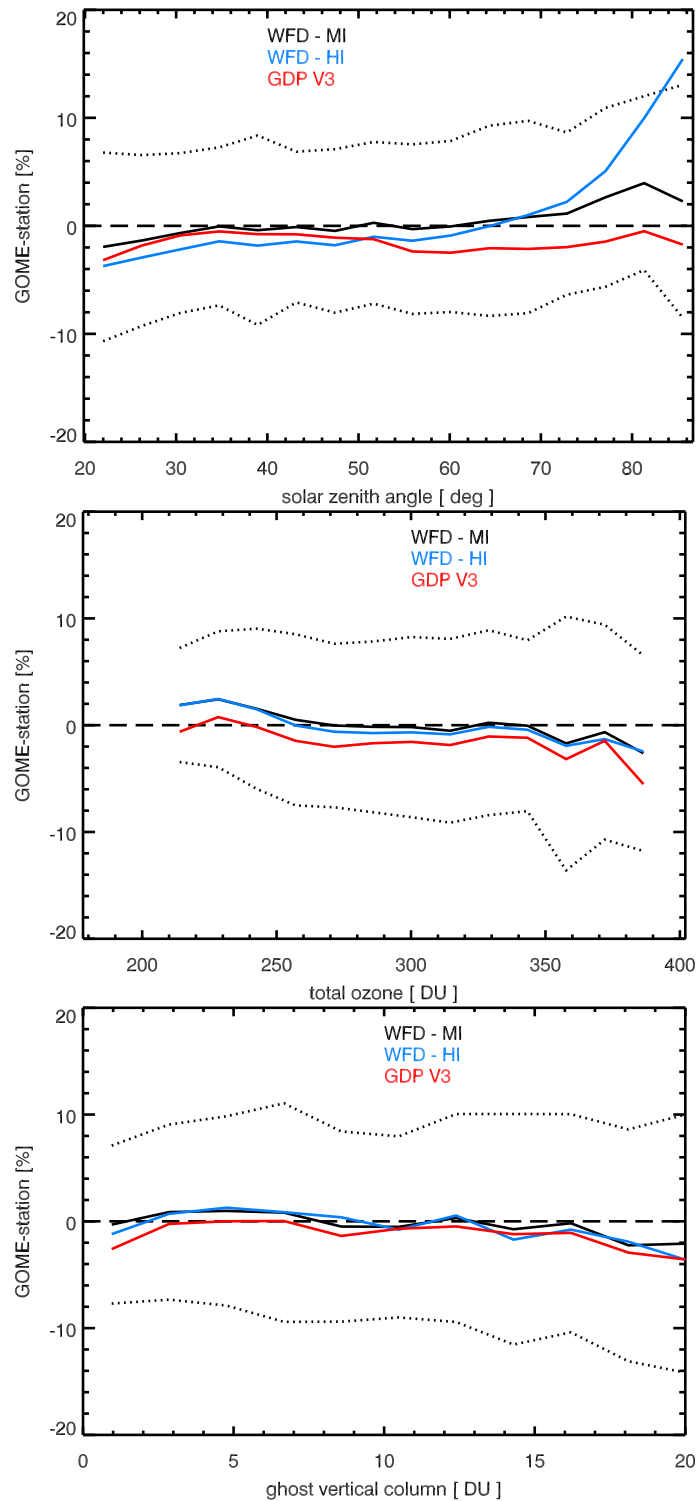


Figure B.8: Statistics on SH mid-latitude stations (six stations). Top: as a function of GOME solar zenith angle. Middle: as a function of total ozone. Bottom as a function of the ghost vertical column.

B.5 Southern polar region, 60°S-90°S

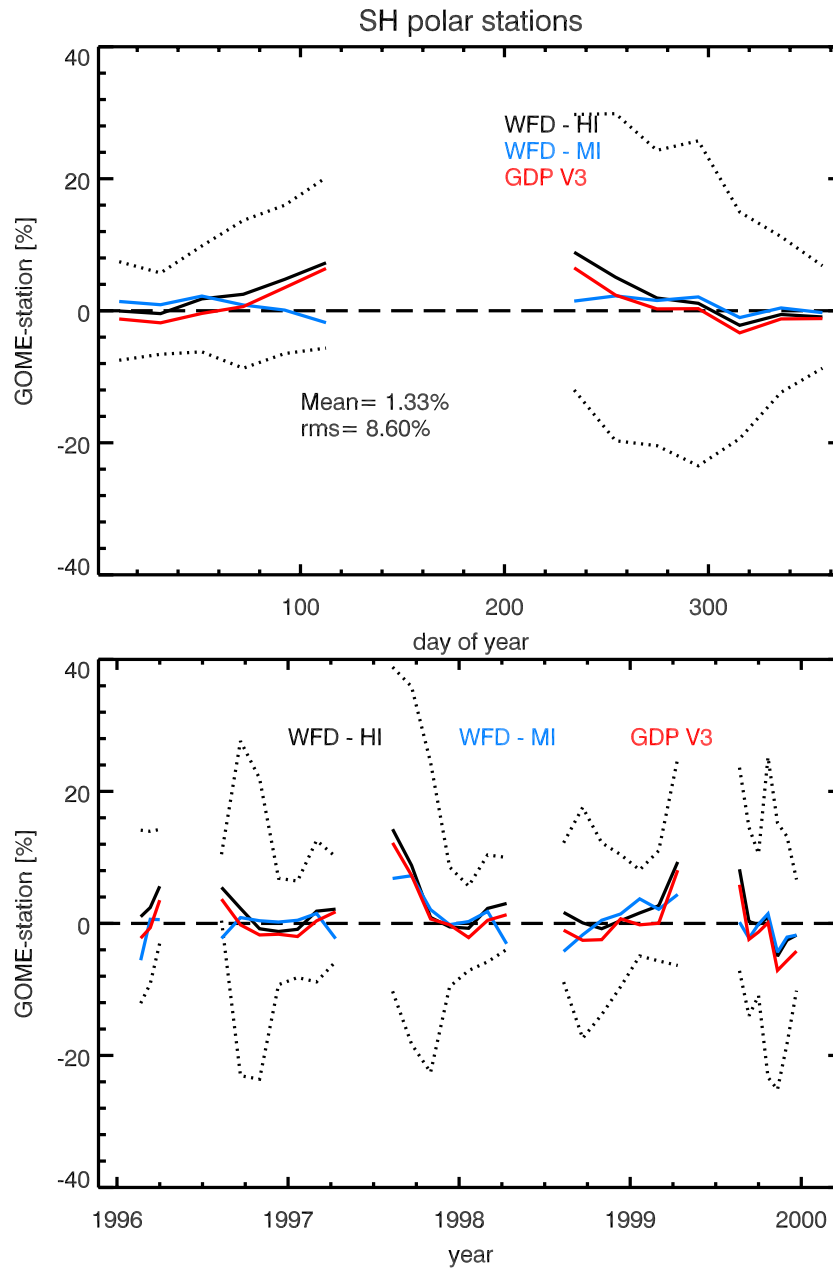


Figure B.9: Statistics on SH polar stations (four stations). Top: as function of day in year. Bottom: as a time series from 1996 to 1999. The lines mark seasonal averages (three month) and the dotted lines are the 2σ RMS in the observed differences (WF-DOAS with default TOMS V7 climatology).

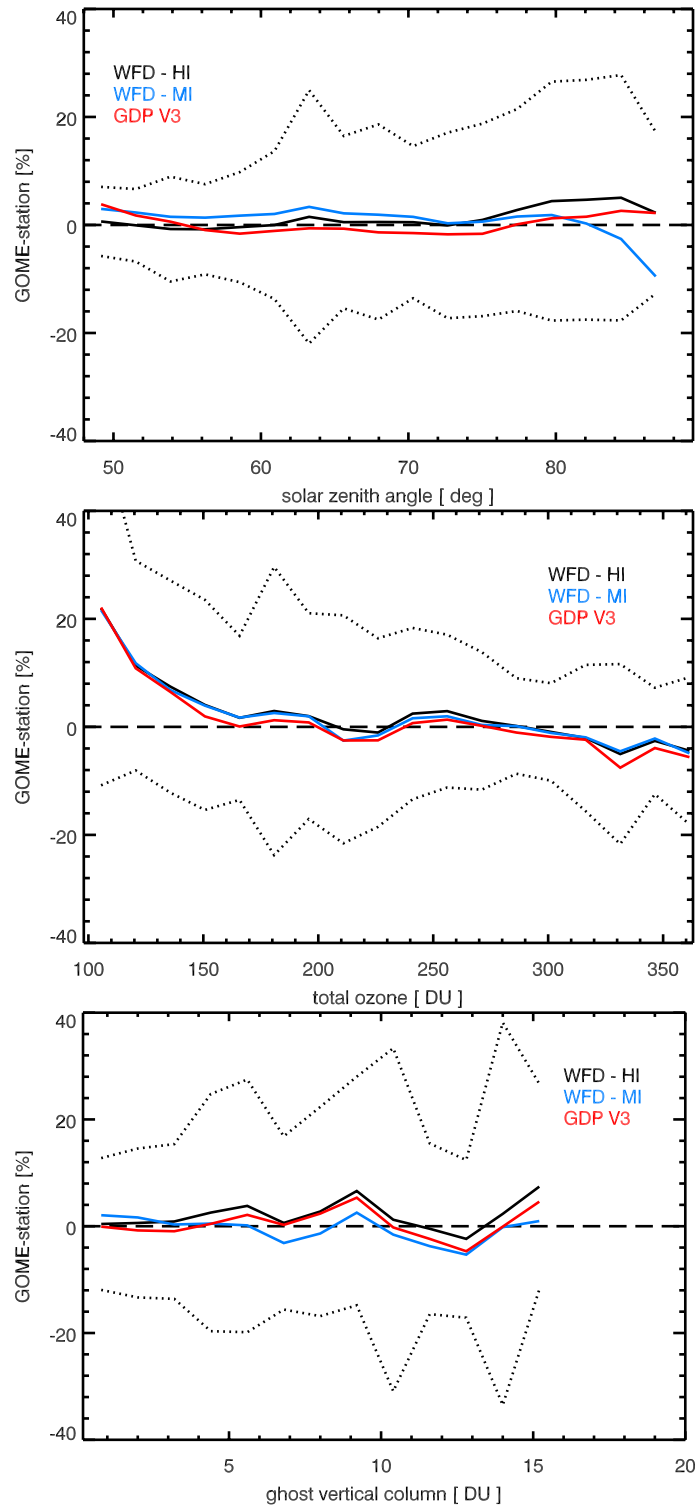


Figure B.10: Statistics on SH polar stations (four stations). Top: as a function of GOME solar zenith angle. Middle: as a function of total ozone. Bottom as a function of the ghost vertical column.